Role of Mitochondria in Ischemia / Reperfusion Mediated Brain Injury: Mechanisms and Pharmacological Interventions

Dissertation

zur Erlangung des akademischen Grades

doctor rerum naturalium (Dr. rer. nat.)

von M.Sc. Syed Shaida Ahmad Andrabi
geb. am March 1, 1974 in Pulwama, Kashmir, Indien

genehmigt durch die Fakultät für Naturwissenschaften der Otto-von-Guericke-Universität Magdeburg

Gutachter:

Prof. Dr. Gerald Wolf, Magdeburg
PD Dr. Ingolf Blasig, Berlin
PD Dr. Lorenz Schild, Magdeburg

eingereicht am: April 28, 2004
Verteidigung am: December 14, 2004

Role of Mitochondria in Ischemia / Reperfusion Mediated Brain Injury: Mechanisms and Pharmacological Interventions

Thesis

for the award of the academic degree

doctor rerum naturalium
(Dr. rer. nat.)

corresponding to Doctor of Philosophy
(Ph. D.)

by Syed Shaida Ahmad Andrabi, M.Sc.,

born on March 1, 1974 in Pulwama, Kashmir, India

Approved by

The Faculty of Natural Science

Otto-von-Guericke University Magdeburg, Germany

Reviewers:

Prof. Dr. Gerald Wolf, Magdeburg
PD. Dr. Ingolf Blasig, Berlin
PD Dr. Lorenz Schild, Magdeburg

Submitted on: April 28, 2004

Defense on: December 14, 2004

To the loving memories of my belated uncle, who taught me to look beyond, what the world can see

Long gone but never forgotten

A C K N O W L E D G E M E N T

I am highly indebted and grateful to the mentor of my research carrier, Prof. Dr. Gerald Wolf, for providing me an opportunity to work under his esteemed guidance at the Institute for Medical Neurobiology. His constant inspirations, inestimable motivations, uncompromising regulations, professional guidance, love and care made it possible for me to expedite my task smoothly and efficiently.

How to express my gratitude to Dr. Thomas FW Horn for supervising all of my research work. His excellent scientific inputs and sincere efforts enabled me to compile my Ph.D thesis successfully. The experience I gained under his dedicated and disciplined scientific environment will be my life-long asset and an invaluable reward. I will ever remain indebted to him.

My sincere thanks goes to Prof. Dr. Detlef Siemen for his valuable scientific advices, support and encouragement during the course of my study. I am also thankful to Dr. Iqbal Sayeed, who helped me in carrying out the Patch Clamp experiments in Prof. Siemen's Laboratory.

I acknowledge with gratitude the inspirations, scientific advices and moral support extended by PD Dr. Mario Engelmann.

My special and sincere thanks are reserved for Heike Baumann for her excellent technical assistance and for being available at odd hours for the successful completions of my experiments.

Labmates and colleagues are true companions, without whom a researcher is incomplete. I had the privilege of having Dr. Mariarosa Spina and Aileen Schröter, who were always by my side with all their support, help and encouragement. I share all of my happiness and satisfaction with them. I am also grateful to Alexander Goihl, Dr. Yuliya Dahlem, Gabriella Orlando, Dr. Sanjoy Roychoudary, Dr. Peter Lorenz and Iveta Joroscakova for their help and support.

ACKNOWLEDGEMENT

I am highly thankful to PD. Dr. G. Keilhoff, Dr. F. Rothe, Dr. K. Richter, Dr. K. Langnaese for their help and support during the entire course of my study

My special thanks also goes to Andrea Rudloff, Karla Klingenberg, Monika Michaleck, Rita Murau, Regina Dobrowolny, Irmgard Leschka, Gudrun Schmidt, Renate Lüddecke and Leona Bück for their help and co-operation.

How could I forget the constant help and moral support extended by Julia Czerney and Beate Zörner. I will always remain grateful to both of them.

Those, who were not directly involved in my scientific research but share a major portion of satisfaction and happiness for my achievements, are my beloved parents, sisters and all of my relatives. I hereby offer my proud salutations to all of them for their love and encouragement. Their belief in me, gave me the energy to move on.

CONTENTS

1. INTRODUCTION

Stroke-related brain injury is a major cause of mortality and severe neurological disability. In practice, stroke refers to a range of conditions that are caused by occlusion or hemorrhage of one of the main arteries supplying blood to cerebral tissues. Ischemia is simply defined as the diminution of cerebral blood flow (CBF) to a critical threshold that propagates brain damage. Focal cerebral ischemia entails reduction in CBF to a specific vascular territory, usually encountered clinically due to thrombotic, embolic or hemorrhagic strokes [1]. The tissue in the center of the ischemic area with severe CBF reduction, is termed as ***ischemic core***. Distal from the ischemic core towards the regions where the blood flow is normal, the ischemic injury becomes progressively less severe. This peripheral region of the ischemic territory in which the blood flow reduction is less severe, corresponds to the so-called ***ischemic penumbra***. The relative maintenance of perfusion in the ischemic penumbra is the result of collateral blood flow operating from the adjacent non-ischemic territory (for review, see [2]). The majority of strokes are a result of focal ischemia and one of the major blood vessels affected is the middle cerebral artery (MCA) [3]. Another cause, global cerebral ischemia, involves a reduction or absence of CBF to the entire brain, situations usually encountered in severe hypotension or acute cardiac arrest [1]. In all cases, the stroke ultimately involves dysfunction or death of brain cells, giving rise to cerebral infraction. Depending on the location and size of the infarct, stroke may lead to neurological deficits or in severe cases, death of the subject.

The primary event during ischemia is the inhibition of the electron transport chain and hence, oxidative phosphorylation because of reduced supply of oxygen and glucose to the affected tissue. This fall in respiration is followed by a rapid decrease in adenosine triphosphate (ATP) levels [4]. Consequently ATP-dependent elements, such as the Na^+ pump is inhibited, causing an imbalance in Na^+ / K^+ ion concentrations and a membrane depolarization in the cells of affected cerebral tissue [5]. These changes are very dramatic during global ischemia and also in the core of focal lesions. However, such changes are much less severe in the penumbra of focal lesions [6]. In the penumbra, the levels of ATP do not fall nearly as much as in global ischemia or the core. All these events initiate the pathways of cell death in stroke.

1.1 Cell death in cerebral ischemia

The characterization of the cell death pathways in stroke is of primary importance to develop therapeutic interventions. Cell death in ischemia has traditionally been considered as “necrotic”. During the last decade, research has revealed that apoptosis equally contributes to the ischemic cell death [7-9]. Apoptosis is an energy dependent pathway that involves an active proteolytic process, which leads to nuclear and cytoplasmic condensation, intra-nucleosomal DNA fragmentation and cell compartmentalization into apoptotic bodies that are engulfed by neighboring macrophages [10, 11] The phagocytic action of macrophages rapidly remove the apoptotic cells, without eliciting an inflammatory reaction. In contrast, necrosis results from energy depletion, dissipation of ionic gradients, cell swelling, disruption and permeabilisation of the plasma membrane and loss of intracellular contents, leading to inflammatory response [12].

In ischemia, the involvement of apoptotic cell death is now widely accepted, however, questions arise from the fact that the morphological features of ischemic cell death do not correlate with the molecular markers of apoptosis. Two main hypothesis have been proposed to reconcile the biochemical and morphological evidences of ischemic cell death. The first is that ischemic cell death may proceed via a number of pathways with similar operative mechanisms, which lead to apoptosis as well as necrosis [13, 14]. Such common mechanisms include excitatory amino acid release and ionic imbalance that contribute to both apoptosis and necrosis. An alternative hypothesis is based on the concept that apoptosis may be masked by necrosis under ischemic conditions [15, 16]. *In-vitro* studies have provided examples of shifts from apoptosis to necrosis and vice versa [17-19]. In ischemic tissue, the energy levels in the infarct core approach zero [20] but respiration is maintained, at least partially, in the penumbra by collateral reperfusion from adjacent arteries, providing a suitable environment for neuronal apoptosis to fully occur. Although many morphological and biochemical observations of the ischemic cells have been made during the late stages of infarction [12], the neurons of the so called necrotic core display features of apoptosis [12]. Caspase activation, apoptotic DNA fragmentation and dilation of endoplasmic reticulum (ER) have been observed in cerebral infarctions [12, 21, 22]. Thus, apoptosis is indeed being triggered by ischemia but as the availability of the cellular energy declines, apoptotic degenerative processes are replaced by necrotic processes [12]

In ischemic tissue, electron microscopic studies revealed mixed markers for both apoptosis and necrosis within the same cell [23]. These studies indicate that there is a co-existence of apoptosis and necrosis in ischemic tissue. The main stream executors of apoptosis are ***Caspases*** that consist of a family of proteases which possess a cysteine-containing pentapeptide catalytic site and require an aspartate residue at the N-terminal end of the substrate cleavage site. Caspases are synthesized as inactive proenzymes (procaspases) that comprise an N-terminal prodomain, a large and a small subunit. Activation results from proteolytic cleavage of the procaspase into its three component parts, usually mediated through the action of other activated caspases. Subsequently, two large and two small subunits associate to form the heterotetrameric active enzyme. Caspases can be divided into two groups, the initiator caspases (-2, -8, -9 and -10) and the effector caspases (-3, -6, and -7) [24, 25]. The initiator caspases have long prodomains that interact with the death domains (DDs) of other transmembrane and intracellular proteins and through these interactions, transduce a range of pro-apoptotic stimuli into proteolytic activity [24-26]. The effector caspases have short prodomains and are directly responsible for the cleavage of cellular substrates, causing most of the morphological and biochemical features of apoptosis. Substrates which are degraded or inactivated by caspase-mediated cleavage include cytoskeletal proteins such as actin, α-fodrin, and gelsolin, structural nuclear proteins such as the lamins, poly(ADP-ribose) polymerase (PARP) [25, 27], anti-apoptotic proteins Bcl-2 and Bcl-xL**,** and the inhibitor of caspase-activated DNase (ICAD) [28, 29]. The cleavage of ICAD releases caspase-activated DNase (CAD) and leads to the apoptotic cleavage of nuclear DNA [28, 29].

There is a large body of evidence that brain ischemia can cause an activation of caspases. Up-regulation and activation of caspase-3 was found to precede the neuronal death, especially in the hippocampus and caudate-putamen in focal and global models of cerebral ischemia [30-32]. Cao at al. [33] reported that transient global ischemia in the rat caused caspase-3-mediated cleavage of ICAD, resulting in the apoptotic degradation of DNA by CAD. Luo et al. [34] found that deoxyribonuclease activity in transient focal ischemia could be prevented by inhibitors of caspase-3.

The mRNA and protein levels of several procaspases like -3, -6 and -8 were found to increase in focal brain ischemia [35]. Also, an activation of caspases-3, -8 and cleavage of PARP was observed in the ischemic cerebral tissue [35]. Several studies have shown that intra-cerebroventricular injections of selective caspase inhibitors are neuroprotective in

transient [36-38] and in permanent ischemia [35]. The caspase activation and, hence apoptosis execution is carried out by two main pathological processes: the mitochondrial and the death receptor-mediated pathways (for review, see [39]).

1.2 Mitochondrial pathway of apoptosis

The mitochondrial pathway of apoptosis plays a pivotal role in ischemia / reperfusion injury [39]**.** This pathway of cell death is initiated by the release of intramitochondrial proteins, such as cytochrome c (cyt c), apoptosis-inducing factor (AIF) and smac / DIABLO into the cytosol [40]. A number of mitochondrial changes have been observed that lead to release of these substances, which include alterations in mitochondrial membrane permeability, largely attributed to the formation of mitochondrial permeability transition pore (mtPTP) and disruption of the mitochondrial membrane potential ($\Delta\Psi m$) [41]. Some contradicting studies on isolated mitochondria suggest that the release of cyt c might occur also independently of the mtPTP. For example, Andreyev and Fiskum [42] showed that mtPTP-mediated cyt c release was found in liver but not in brain mitochondrial suspensions. The discrepancy between these studies is not fully understood. It was suggested that the induction of mtPTP opening and subsequent cyt c release from brain mitochondria might require the intact tissue [42].

Translocation of proapoptotic proteins like BAX, Bid, forming oligomeric channels in the mitochondrial membranes, is also one of the mechanisms for release of proapoptotic factors from the mitochondria (for review, see [43]). The occurrence of such events is well documented in experimental models of transient and permanent ischemia [44-48]. A universally recognized role of mitochondria in death signaling is the release cyt c from the mitochondrial intermembrane space, which is a 13 kD nuclear encoded protein that is highly conserved among species and functions as an electron carrier in the electron transport chain of mitochondria. It is translocated from cytosol as an unfolded apoprotein (apo-cyt c), which contains an integral rather than an N-terminal mitochondrial targeting signal, as it is usually the case with most other proteins imported into the mitochondria from the cytosol [49]. Only holo-cyt c, containing covalently bound heme (but not apo-cyt c that has no heme attached) is competent to carry out the apoptotic signaling [50]**.** The pro-apoptotic role of cyt c is conferred by its interactions with cytosolic factors, which include apoptotic protease-activating factor-1 (apaf-1) and caspase-9. Following release of cyt c into the cytosol, apaf-1 as well as procaspase-9 are recruited to it, generating a

complex, the apoptosome [51-53]. cyt c is critical in this process as in its absence, apaf-1 is unable to bind procaspase-9 [51-53]**.** In this complex, the pro-caspase-9 ultimately gets cleaved and thereby activated [51-53]. Active caspase-9, in turn, activates caspase-3, which then initiates the process of apoptotic cell death by inducing DNA fragmentation via activation of a DNA breaking enzyme, the CAD [28, 29].

1.3 Oxidative and nitrosative stress

The cascade of events in the pathogenesis of stroke involves oxidative and nitrosative stress, i.e., the deleterious effects of reactive oxygen and nitrogen species (ROS / RNS) [54-56]. The overload with these substances that include hydroxyl radicals ($^{\cdot}OH$), superoxide anions ($O_2^{\cdot-}$), hydrogen peroxide (H_2O_2), nitric oxide (NO) and peroxynitrite ($OONO^-$) is known to promote DNA damage, peroxidation of lipids, proteins, and carbohydrates, blood brain barrier break-down and microglial infiltration into the ischemic territory (for review, see [55, 57]). ROS / RNS are considered as upstream triggers of mitochondrial damage [58, 59] by inducing the release of cyt c [58, 60]. In ischemia / reperfusion, the production of ROS / RNS is particularly significant during reperfusion phase [61, 62]. ROS / RNS cause acerbated mitochondrial damage by depleting pyridine nucleotides and glutathione, two reducing components that protect mitochondria from oxidative damage.

There are multiple pathways whereby ROS / RNS are produced in the brain. The $O_2^{\cdot-}$ radicals are produced by electron leakage from the electron transport chain in mitochondria and by oxidation of hypoxanthine to xanthine and urate by xanthine oxidase. Other sources of ROS / RNS include degradation of free fatty acids by phospholipase A_2 into arachidonic acid and subsequent oxidation of arachidonic acid by cyclooxygenase and lipooxygenase. NADPH oxidase activity in macrophages, neutrophils, and microglia also contribute to ROS / RNS production [63].

Production of NO occurs through conversion of arginine to citrulline by three different nitric oxide synthases (NOS): neuronal NOS (nNOS), endothelial NOS (eNOS), and macrophage or inducible NOS (iNOS). NO is a vasodilator but it is also a free radical that binds to iron and thiol groups of proteins, including metabolic enzymes. It can cause nitrosative or oxidative stress when generated in excess amounts. NO can exert its pathological effects either by directly acting on its targets or indirectly after combining with other reactants. NO cytotoxicity may cause s-nitrosylation of important cytosolic thiol

proteins, it induces lipid peroxidation, respiratory chain complex inhibition and mitochondrial impairment (for review, see [64]) The inhibition of respiration could contribute to the pro-apoptotic effects of NO by membrane potential reduction, ensuing activation of the mtPTP and release of pro-apoptotic factors from the mitochondria. $NO^{\cdot}$ and $O_2^{\cdot -}$ react very quickly to form $ONOO^-$. The $ONOO^-$ is freely diffusible in its protonated form, oxidizes thiol groups, induces protein nitrosylation, mitochondrial impairment, and decomposes into $^{\cdot}OH$ and NO_2 [65]. High Ca^{2+}, high ADP in ischemia / reperfusion stimulate excessive mitochondrial $O_2^{\cdot -}$ release, as does the addition of NMDA to the cell cultures [66].

In normal brain tissue ROS / RNS are detoxified by endogenous enzymatic and non-enzymatic antioxidants including superoxide dismutase (SOD), glutathione peroxidase, catalase, thioredoxin and glutathione [56, 67-69]. When the production of ROS / RNS exceeds this endogenous defense capacity, oxidative / nitrosative stress injury ensues (for review, see [56, 70, 71]). Mitochondria appear to be both a site of ROS production as well as a target of ROS / RNS attack. Mice overexpressing the mitochondrial manganese superoxide dismutase (Mn-SOD) displayed less tissue damage and cyt c release after focal ischemia than wild-type animals [72]. Consistently, mice with a partial deficiency of the Mn-SOD gene displayed increased cytochrome c release and more extensive tissue damage [47, 73, 74].

There is a large body of evidences showing that ROS / RNS are generated after ischemia / reperfusion and that they play an important role in the development of brain injury [75-77]. It was shown that inhibitors of lipid peroxidation, xanthine oxidase and ROS scavengers or iron chelators reduced brain damage [77-79]. Several studies suggest that NO is produced in excessive quantities after ischemia / reperfusion and pharmacological blockade as well as knock-out mice lacking NOS have reduced the cerebral ischemic damage [80, 81]. Hence, the concept of pharmacological supplementation against ROS / RNS with antioxidants has become an area of intense research (for review, see [82, 83]).

1.4 Excitotoxicity

Glutamate, the major excitatory neurotransmitter in the brain, plays an important role in excitotoxicity. It acts in about 30% of synapses in central nervous system (CNS), it is kept in specific vesicles and is released in little doses that take over the receptors and then is metabolised by specific enzymes. The sequence of excitotoxicity starts with the excessive

extracellular accumulation of glutamate. Extracellular levels of glutamate in experimental models of stroke has been reported to increase after ischemic insults [84]. In agreement with this, it was shown that a blockade of glutamate receptors reduce the brain infarction in cerebral ischemia [85]. Glutamate acts on three families of receptors (for review, see [86, 87]). One family of these receptors (NR1, NR2A, NR2B, NR2C and NR2D) is activated by glutamate analogue *N*-methyl-*D*-aspartate (NMDA) and collectively referred to as NMDA-receptors [86]. Another family of the glutamate receptors includes α-amino-3-hydroxy-5-methyl-4-isoxalone propionic acid (AMPA) and kainate receptors, which are activated by AMPA and by kainate respectively. These two families of glutamate receptors are collectively called as ionotropic glutamate receptors as they are directly linked to ion channels. The third family of glutamate receptors consists of G-protein coupled receptors, the so-called metabotropic receptors, which are subdivided into group I (mGluR1 and mGluR5), II (mGluR2 and mGluR3), III (mGluR4, mGluR6, mGluR7 and mGluR8) (for review, see [86]). NMDA receptor over-stimulation in relation to excitotoxicity is very well studied. For the stimulation of NMDA receptors by glutamate, glycine acts as a co-agonist. The co-agonistic binding of glycine is important for this receptor to be stimulated by glutamate. Its stimulation causes the entry of Ca^{2+} into the cells as it is directly linked to Ca^{2+} channels. Under normal conditions the cytosolic Ca^{2+} ($[Ca^{2+}]_c$) is stable and low, around 10,000 times lower than the extracellular level. But in pathological conditions like ischemia / reperfusion, the over-stimulation of the NMDA receptor causes increased entry of Ca^{2+} into the cells thereby mediating the excitotoxicity and neuronal damage. The excess of $[Ca^{2+}]_c$ is highly toxic for the cells, promoting cerebral edema formation and activation of intracellular self-destruction cascade.

Ca^{2+}, a cellular messenger that controls important aspects of cell and tissue physiology, can be turned into death signals when delivered at a wrong time and at a wrong place [88, 89]. Mitochondria eventually decide whether Ca^{2+} signals are decoded as life or death [90]. Scorrano et al. [91] demonstrated that transfer of Ca^{2+} from ER to mitochondria is required for initiation of programmed cell death by some, but not all apoptotic signals. The role of Ca^{2+} as a death trigger was first suggested by Fleckenstein et al., who proposed that the entry of excess of Ca^{2+} into myocytes might be the mechanism underlying the cardiac pathology that occurs after ischemia [92]. Subsequent studies emphasized the general importance of this observation as both receptor over-stimulation [93] and cytotoxic agents [94] were found to cause influx of Ca^{2+} into the cells. It is now known that Ca^{2+} dependent

processes are interwoven with the main stream apoptosis executors, the caspases and recent findings indicate that interfering with the sequestration of Ca^{2+} into intracellular pools can be sufficient to trigger apoptosis [95]. Ca^{2+} overload and Ca^{2+} dependent processes have been shown to activate and modulate the execution of non-apoptotic cell death as well [96].

1.5 Mitochondrial Ca^{2+} and permeability transition pore

Mitochondria are known to actively participate in $[Ca^{2+}]_c$ regulation [97]. Mitochondria act as Ca^{2+} buffers in the cells by sequestering excess of Ca^{2+} from the cytosol. However, if the intramitochondrial Ca^{2+} reaches a certain threshold level, it becomes detrimental. [98, 99]. Ca^{2+} enters the mitochondria by the electromotive force, driven by the mitochondrial membrane potential ($\Delta\Psi_m$). According to the chemioosmotic theory of Mitchell [100], the electron transport in the respiratory chain of mitochondria causes the extrusion of H^+, creating a large electrochemical difference across the inner mitochondrial membrane that creates the $\Delta\Psi_{m.}$. The potential generates a net negative charge inside the mitochondria that entails the driving force for the Ca^{2+} to enter into the mitochondria. Ca^{2+} enters mitochondria via the Ca^{2+} uniporter and exits by exchange with Na^+ on the Na^+ / Ca^{2+} carrier; thereby maintaining a continuous Ca^{2+} cycling across the mitochondrial membranes (Fig. A) [101, 102]. The continuous Ca^{2+} cycling maintains the physiological mitochondrial Ca^{2+} pool low. However, under pathological conditions like neuronal death, the intracellular Ca^{2+} get accumulated in higher amounts, thereby exposing the mitochondria to high Ca^{2+} concentrations [97]. Exposure of mitochondria to high Ca^{2+} makes them to buffer much higher amounts of $[Ca^{2+}]_c$ that in turn causes mitochondrial swelling and release of intra-mitochondrial contents into the medium [98, 99]. This pathological process disrupts the mitochondrial Ca^{2+} cycle and results in a faulty handling of Ca^{2+} by mitochondria. It is now realized that this sequence of events reflects the assembly of a proteinacious pore, called the mitochondrial permeability transition pore (mtPTP) [96].

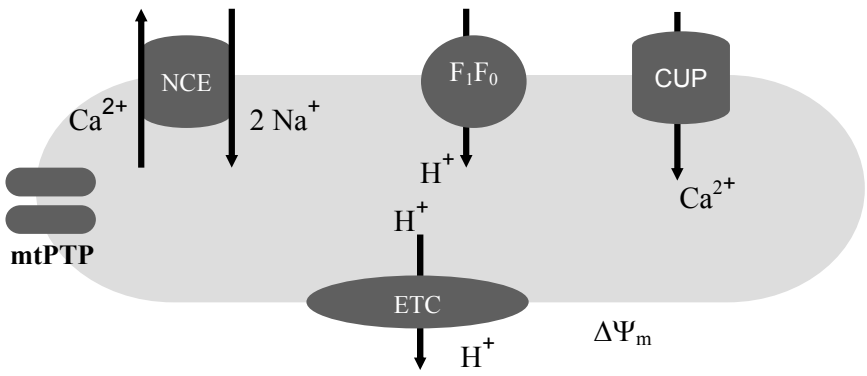

Fig. A: Figure showing the transport of Ca^{2+} and H^+ inos across the inner mitochondrial membrane (**NCE:** Na^+ / Ca^{2+} exchanger; **F_1F_0:** F_1F_0 ATP synthase; **CUP:** Ca^{2+} uniporter; **ETC:** electron transport chain.)

mtPTP allows the release of accumulated Ca^{2+} as well as of various low and high molecular weight compounds from the mitochondria. This process is accompanied by osmotic swelling of the mitochondria, collapse of ٨Ψm and to the cessation of ATP generation. Additionally, the pore formation leads to bursting of mitochondrial membranes and production of reactive oxygen species (ROS). Thus, the mtPTP formation represents a fundamental pathological process that can initiate pathway of cell death, either by causing ATP depletion and energetic collapse [41] or by promoting the release of mitochondrial proteins including cyt c that leads the cells into apoptosis (for review, see [59, 103, 104]). It is reported that decrease in ATP, oxidative stress and calcium accumulation are the major factors that trigger the assembly of mtPTP [105, 106], however high Ca^{2+} and oxidative stress have emerged as major determinants for mtPTP formation [107, 108].

1.6 Molecular composition of mtPTP

The molecular composition of mtPTP remains uncertain. The dominant hypothesis is that the mtPTP spans the mitochondrial inner and outer membrane and is composed of proteins from both the membranes and the matrix (Fig. B). Inhibitor and reconstitution studies implicate that the adenine nucleotide translocase (ANT), located in the inner mitochondrial membrane (IMM), is an essential component of the mtPTP [59]. Atractyloside that binds to ANT from the cytosolic side induces the pore formation, whereas bongkrekic acid that binds to ANT from matrix side, blocks the mtPTP [59]. Recent studies on ANT knock out mice showed that mtPTP assembly can also occur without ANT. Voltage-dependent anion

channel (VDAC) or porin of the outer mitochondrial membrane (OMM) complexes with ANT forming the core component of the mtPTP [109, 110]. A critical factor in the induction of mtPTP is the interaction of Cyp D to the VDAC-ANT complex. Cyp D is a 18 kD mitochondrial matrix protein that translocates from matrix to mtPTP during conditions of high Ca^{2+} and oxidative stress [59]. Immunosuppressant cyclosporine A (CsA), has been proved to be a strong inhibitor of mtPTP. This is presumably because CsA binds with Cyp D, thereby blocking the mtPTP by competing with the effects of Ca^{2+}-cyclophylin for occupancy on the transition pore complex [105]. CsA also inhibits the cytosolic immunophilin calcineurin. Immunosuppressant FK-506, that inhibits calcineurin but not Cyp D, has no effect on mtPTP. Furthermore, an analogue of CsA, N-methyl-valine-4-cyclosporine that has no effect on calcineurin but readily inhibits the mtPTP. Other proteins associated with the pore that are know to increase the pore conductance, include hexokinase, creatinine kinase, the peripheral benzodiazepine receptor and pro-apoptotic proteins like BAX [59].

The mtPTP inhibitor CsA is protective in various models of cerebral ischemia *in-vitro* and *in-vivo* [111-113], suggesting that the inhibition of mtPTP comprises a target for pharmacological intervention to prevent cell death in cerebral ischemia.

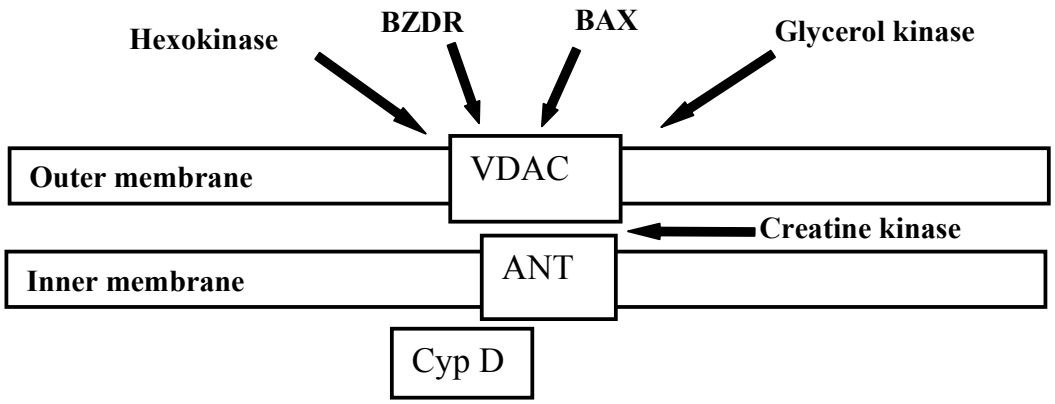

Fig. B: The basic unit of the PT pore is the VDAC–ANT–Cyp-D complex located at contact sites between the mitochondrial inner and outer membranes. Other proteins associate with the complex as indicated **(Modified from: Crompton, M; Biochem. J. (1999) 341, 233-249)**

(**VDAC**: Voltage dependent anionic channel; **ANT**: adenine necleotide translocase; **Cyp D**: cyclophilin D; **BZDR**: benzodiazepine receptor)

1.7 Pharmacological intervention in cerebral ischemia

Despite substantial research into neuroprotection and a remarkable number of positive results from different laboratories using rodent models, no neuroprotective agent has been conclusively shown to be clinically effective in acute stroke [114]. Except for thrombolytic therapy, which is applicable only in a certain cases of stroke [115]**,** current clinical management is limited to supportive measures and stroke therapy is at the same stage of neuroprotection as 20 years ago. The failure of neuroprotective drugs in clinical situations has been tentatively attributed to several factors that include: (a) difficulty in finding clinically relevant delivery system to administer compounds intracerebrally over a long period of time (b) difficulty in transposing different experimental settings to human situations that are characterised by extreme heterogeneity in the etiology, location and severity of ischemic strokes (c) lack of experimental evidence for long term protection.
The development of new therapeutic strategies remains a crucial challenge. The cell death pathways, necrosis and apoptosis can no longer be categorized as two exclusive pathways in ischemic. It is believed that apoptosis in ischemia is masked by necrotic cell death [15, 16], so the inhibition of early apoptosis seems to be a potential target to attenuate cellular loss in cerebral ischemia. Since, several pathways leading to cell death are activated in cerebral ischemia, effective neuroprotection might require a combination of drugs that target distinct pathways during the evolution of ischemic cell death. Rational therapy based on inhibiting multiple cell death mechanisms might ultimately prove successful in neuroprotection. Also newer mechanisms for neuroprotective actions of well acknowledged neuroprotectants need to be explored that will make it easy to employ effective drug combinations for therapeutic interventions. Also, search for newer neuroprotectants may prove beneficial in stroke therapy.

1.7.1 Melatonin

Melatonin, the main secretory product of the pineal gland, is well known for its neuroprotective effects that are currently attributed mainly to its free radical scavenging and antioxidant properties [116]. Melatonin as a neuroprotectant represents a rational approach to stroke treatment and offers a number of potential advantages. It is highly effective in preventing neuronal loss in models of brain damage where oxidative stress is

involved. The endogenous compound that readily crosses the blood-brain barrier (for review, see [116]) was accordingly found to reduce the infarct size and neuronal injury in experimental ischemia [117-120]. Furthermore, melatonin reduces oxidative stress and rescues dopaminergic neurons in different models of Parkinson's disease [121, 122]. Melatonin protects against the seizures induced by kainate, glutamate and NMDA [123]. Supporting the role of melatonin as an endogenous protectant, an aggravation of brain damage after ischemia or excitotoxic seizures has been reported in rats that are deficient in melatonin production [120]. Besides the direct antioxidant potential, several other mechanisms such as interactions with calmodulin [124] are also considered to be involved in the melatonin mediated neuroprotection. Melatonin is furthermore reported to directly alter the activities of detoxifying enzymes, thereby improving the total antioxidant defense capacity of the cells. Thus, systemic treatment with melatonin has been shown to cause an increase in the glutathione peroxidase activity in rats [125] as well as the gene expression of antioxidant enzymes including Mn-SOD and Cu/Zn-SOD [126]. Moreover, melatonin prevents the activation of the transcription factor NFκB [127]. This may be the underlying mechanism by which melatonin reduces the expression of the iNOS [128], a major source of deleterious reactive nitrogen species like NO or its metabolite $ONOO^-$.

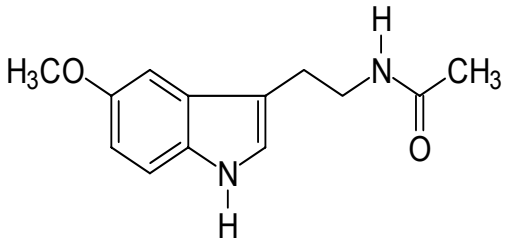

MELATONIN

1.7.2 Oxyresveratrol

Hydroxystilbenes, naturally occurring polyphenolic compounds, are well-known for their free radical scavenging properties [129-131]. Resveratrol, a representative of this group, has been widely investigated for its cytoprotective effects in various pathological models including experimental cerebral ischemia [132, 133]. Recently it was reported that the likewise naturally occurring analogue *trans*-2, 3', 4, 5'-tetrahydroxystilbene, oxyresveratrol (OXY) is a potent antioxidant [131]. Oxyresveratrol is ready available from mulberry wood (*Morus alba* L.) Despite its better solubility in aqueous solutions and less cytotoxicity, yet it is pharmacologically less investigated. Moreover, research has shown that OXY is transported into tissues at high rates resulting in a bioavailability of about 50% [134] OXY, used as an active compound in dermatology [135, 136] is known to inhibit DOPA oxidase activity [137] and cyclooxygenase [137, 138]. It effectively scavenges H_2O_2, NO and the artificial free radical 2,2-diphenyl-1-picrylhydrazyl (DPPH) [131]. Moreover, it was shown that OXY selectively kills activated microglia [131] that are assumed to aggravate the outcome of cerebral ischemia by a high NO-output pathway and the release of cytokines [139]. Such properties and its high solubility in aqueous solutions and low general toxicity, makes OXY potentially superior to resveratrol for neuroprotective studies.

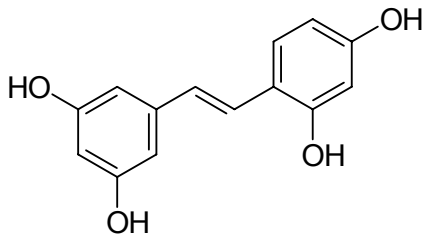

OXYRESVERATROL

1.8 AIM OF THE STUDY

1.8.1 The aim of this study is based on our initial finding in striatal neurons that melatonin inhibits the $[Ca^{2+}]_c$ rise after intense NMDA stimulation in a pattern similar to that of CsA. This observation raises the question if mtPTP inhibition is one of the mechanisms that mediate the neuroprotective effect of melatonin. We hypothesized that melatonin directly inhibits the mtPTP and inhibited the mitochondrial apoptotic cascade in transient brain ischemia. To prove this hypothesis following questions were addressed.

(a): Does melatonin inhibits the mtPTP patch currents at single channel level?

(b): Following the hypothesis that an inhibition of the mtPTP by melatonin should also preserve the $\Delta\psi_m$, we tested, if melatonin preserves the $\Delta\psi_m$ in a neuronal cell culture model of ischemia where mtPTP formation is known to be associated with mitochondrial depolarization.

(c): Being an mtPTP inhibitor, melatonin would also block the cyt c release following mtPTP formation thereby inhibiting apoptosis. We tested if melatonin inhibits cellular distribution of apoptotic markers, namely that of cyt c, caspase-3 and apoptotic-DNA fragmentation in a rat transient brain ischemia model.

1.8.2 Oxidative stress is one of the major factors responsible for the evolution of ischemia / reperfusion injury. OXY potentially reduces the load of ROS / RNS by either direct scavenging effects or by inhibiting the microglial activation, which is one of potential sources of NO and its metabolites. In this study, we tested if OXY protects the brain tissue against ischemia / reperfusion injury in a Middle cerebral artery occlusion (MCAO) model of transient brain ischemia in rats. We also test if this naturally occurring antioxidant inhibits the mitochondrial apoptosis in transient brain ischemia, by assessing the cellular distribution of cyt c, caspase-3 and apoptotic DNA fragmentation, the markers of apoptotic cell death.

2. MATERIAL AND METHODS

2.1 *In-vivo* experiments

2.1.1 Animals

All the animal protocols used in this study were in accordance with the Animal Health and Care Committee of the Land Sachsen-Anhalt, Germany. Male wistar rats weighing 300-350 g were used in the present study. The animals were kept under a 12h /12h light/dark cycle and given free access to food and water. The rats were randomly divided into different treatment groups as described below

2.1.2 Surgical procedure for induction of cerebral ischemia

For the induction of cerebral ischemia, the animals were anesthetised with 2 % halothane in 50 % N_2O / 50 % O_2. During the whole surgical period, the body temperature of the animals was maintained at 36.5 ± 0.5 °C by the use of a heating pad, controlled by a rectal probe. Focal cerebral ischemia was induced by the intraluminal suture method [142] as modified by [143]. Briefly, a 3-0 nylon suture (Ethicon, Johnsons & Johnsons Intl, Brussels, Belgium) with its tip rounded by heating near a flame and coated with poly-L-lysine (prepared by dissolving 1mg poly-L-lysine in 1ml of PBS), was introduced into the internal carotid artery through a nick given-in the external carotid artery and advanced 17-20 mm from the common carotid artery bifurcation to block the origin of middle cerebral artery (MCA). The suture was left in place for 2 h while the animals were allowed to wake up. After 2 h of occlusion, the intraluminal suture was gently removed during a brief period of anesthesia to allow reperfusion. In the groups of sham operated rats all surgical procedures except the occlusion of the MCA were performed. The animals were then returned to their cages and given free access to food and water.

2.1.3 Neurological deficit evaluation

The neurological deficits of the animals were evaluated 24h after reperfusion. The neurological scores were given, using two different methods.

Method I: The widely acknowledged method, described by Bederson et al [144] was used. Accordingly following scores were given:

Scores	Criteria
0	Rats that extend both forelimbs towards the floor when suspended by their tail held at 1 meter height from the ground and have no neurological deficit.
1	Rats that consistently flex the forelimb contralateral to the injured hemisphere, posture varies from mild wrist flexion and shoulder adduction with internal rotation of the shoulder.
2	Rats that showed reduced resistance to the lateral push when placed on a coarse plastic coated paper and have neurological deficit 1.
3	Rats that showed circling behavior consistently towards the paretic side and have neurological deficit 1 & 2.

Method II (Spontaneous movements): Spontaneous motor activity (SPMA) was evaluated by placing the rats in their normal environment (cage) and were observed for 5 minutes. The scores were given as follows:

Scores	Criteria
0	Rats moved in the cage and explored the environment.
1	Rats moved in the cage but did not reach all sides and generally hesitated to move.

2 Rats barely moved in the cage and showed postural abnormalities (Curved towards the paretic side).

3 Rats unable to move and have posture curved towards the paretic side.

2.1.4 Infarct assessment

For evaluation of infract volume, 2, 3, 5-triphenyltetrazolium chloride (TTC) staining method was used [145]. The animals were euthanised 3 days after reperfusion, under halothane anesthesia followed by decapitation. The brains were rapidly dissected out and the forebrains were cut into six 2-mm thick coronal sections using a rat brain matrix (Activational Systems Inc. Michigan, USA). The sections were then incubated in a 2% TTC solution (prepared in PBS) at 37 °C for 15 min. The live tissue stained red while the infracted tissue did not stain and remained pale. After TCC staining, the sections were fixed in 10% buffered paraformaldehyde (PFA). The images of the TTC-stained sections were acquired by scanning after 24 h of PFA fixation, by a high resolution scanner (Hewlett Packard Scanjet 6100C/T). The mean infarct area of each section was calculated as the average of the area on the rostral and the caudal side. Total infarct volume was calculated by adding the mean-area of each section and multiplied by 2 mm (thickness of the sections). The volume obtained was expressed in mm^3.

2.1.5 Immunohistochemistry

For assessing the cytosolic changes in apoptotic markers and for assessment neuronal injury at cellular level, immunohistochemical studies were carried out. Accordingly cytosolic changes in cyt c and caspase-3 were studied. Along with cyt c and caspase-s, alterations in the MAP-2 and NeuN, markers for neuronal degeneration were also studied. Subsets of four animals in each group were deeply anaesthetised with a mixture of Domitor and ketamine hydrochloride and were transcardially perfused with 100 ml of saline followed by 300 ml of 4 % paraformaldehyde (PFA) and 0.2% glutaraldehyde in PBS. Following post-fixation in 4 % PFA, the brains were cryoprotected in 0.5 M sucrose for 24 h followed by 1.0 M sucrose for 72 h at 4°C. The brain samples were then cut into 25 μm thick coronal sections and the free floating sections were rinsed with PBS and then

incubated in blocking buffer (10% fetal calf serum (FCS) in PBS with 0.3 % Triton X-100) at room temperature for 1 h to block non-specific binding sites. The sections were then incubated with the primary antibodies (diluted in PBS with 0.3% Triton X-100 and 1% FCS) overnight at 4 °C. The following antibodies were used: rabbit anti-cytochrome c, 1:200 (Santa Cruz Biotechnology, CA, USA), rabbit anti-caspase 3, 1:200 (Santa Cruz Biotechnology, CA, USA), monoclonal anti-MAP 2, 1:1000 (Sternberger, Maryland, USA) and anti-NeuN, 1:500 (Chemicon, CA, USA). Primary antibody binding was detected by incubating the sections with fluorescent conjugated anti-rabbit (1:500, Alexa 546, Molecular Probes, Leiden, Netherlands) or anti-mouse (1:500, Alexa 488, Molecular probes, Leiden, Netherlands) secondary antibodies (diluted in PBS) for 2 h at room temperature. In control sections, the buffer was added instead of primary antiserum. LSM Pascal confocal microscope (Carl Zeiss, Germany) was used for visualisation of the immunostained sections.

2.1.6 Assessment of DNA fragmentation

For assessing DNA fragmentation, a monoclonal antibody (Apostain, Alexis Biochemicals, Grunberg, Germany) was used. The Apostain method was followed as provided by the manufacturer with some modifications. Accordingly, the perfusion fixed brains with 4 % PFA were post-fixed in the same fixative for 24 h and thereafter cut into 25 μm thick frozen sections. The sections were then taken up onto the superfrost slides and heated in 50 % formamide to yield single stranded DNA (ssDNA) fragments. The slides were then incubated with the monoclonal antibody to ssDNA (1:50) for 30 min at 37 °C to label the ssDNA fragments. The primary antibody binding was detected by incubating the sections with horse-radish peroxidase-conjugated IgM rat monoclonal anti-mouse secondary antibody (Zymed, CA, USA, diluted 1:50 in PBS) and counterstained with hematoxyline. The darkly-stained apoptotic cells were visualized in transmission light mode using the LSM Pascal confocal microscope (Carl Zeiss, Germany).

2.2 *In-vitro* experiments

2.2.1 Preparation of primary neuronal cultures

Primary neuronal cell cultures were prepared from mouse embryo-striatum, taken out from 15 days old pregnant mice as described [146]. The mother mice were anesthetised under halothane inhalation and the fetus were taken out of their womb in sterile PBS under a sterile hood. The heads were separated from the body and the brains were dissected out from the foetus heads. The dissected out brains were put in Dulbecco's modified Eagle's medium (DMEM, Sigma Chemicals, Deisenhofen, Germany) containing 10 % fetal calf serum (FCS). Thereafter the striatal regions, free from meninges were taken out from the dissected fetal brains and dispersed in DMEM containing 10 % FCS. After dispersion of the tissue, the FCS containing DMEM was washed with serum free DMEM, supplemented with B27 nutrients (1:50) and streptomycin/ penicillin (1:500). 2ml aliquots of cell suspension were plated on poly-D-lysine coated glass cover slips (22mm) in 35 mm petri dishes at a final density of 3.5 x 10^6 cells per ml. The cells were cultured in an incubator at 37 °C in a humidified atmosphere containing 5 % CO_2 in air.

2.2.2 Preparation of glass cover slips for Neuronal cultures

0.1 % solution of poly-D-lysine was prepared by dissolving 1 mg of poly-D-lysine in 1 ml of 0.15 M boric acid (prepared in PBS). 22 mm glass coverslips were incubated in the poly-D-lysine solution for 1 h and thereafter rinsed with sterile distilled water. The coverslips were then kept for drying in an incubator till use.

2.2.3 Intracellular Ca^{2+} measurements by fluo-4 imaging

Cell cultures were loaded with 2.5 μM fluo-4 AM (Molecular Probes, Leiden, Netherlands, stock solution prepared in a 20 % pleuronic acid in DMSO, for 45 min at 37 °C. After dye loading, the cultures were transferred into a stainless steel chamber (Atto-fluor, 2 mL volume) that was mounted on a thermostatically controlled stage (37 °C) on an inverted confocal laser scanning microscope (AXIOVERT, LSM PASCAL, Zeiss, Germany). Cells were observed using a Zeiss 63x oil immersion lens. For imaging of Ca^{2+}-sensitive fluo-4

fluorescence, excitation light was provided by an argon laser at 488 nm. Fluo-4 fluorescence emission, filtered at 505 nm long-pass, was recorded using the photomultiplier of the LSM Pascal. Image acquisition frequency was set at 1 image per 10 s. Cells were superfused with Hepes-buffered salt solution (HBSS) containing (in mM): 137 NaCl, 5 KCl, 20 HEPES, 10 glucose, 1.4 $CaCl_2$, 3 $NaHCO_3$, 0.6 Na_2HPO_4, 0.4 KH_2PO_4 at pH 7.4, at a rate of 2 ml / min using a peristaltic pump (Gilson). After mounting the cells on the microscope the cultures were superfused for 5 min with HBSS to wash out excess dye. Then the sequential imaging was started and the cultures were further perfused with buffer alone for 100 s to obtain a steady baseline. Cultures were then subjected to a continuous application of 200 μM NMDA (Alexis Biochemicls, Grunberg, Germany). In two other subsets of experiments either CsA (2 μM, Alexis Biochemicals, Grunberg, Germany) or melatonin (100 μM, Sigma Chemicals, Deisenhofen, Germany) was added to the perfusion-buffer 20 s after the onset of the NMDA stimulation. Images from the cultures were collected for 20 min of the NMDA application. Analysis of fluorescence intensity was performed off-line after image acquisition by averaging intensity values within boxes overlying cell somata in the images using the imaging software of the Zeiss LSM. Data were normalized and average image intensities were calculated.

2.2.4 Oxygen-glucose deprivation and mitochondrial depolarization

Cell cultures were subjected to 3 h oxygen-glucose deprivation (OGD) followed by 30 min reperfusion. For this purpose, the culture medium was washed with HBSS buffer to remove all the glucose-containing-medium. Then OGD was initiated by changing the medium of the cultures to glucose-free DMEM (Gibco Invitrogen, Karlsruhe Germany) that was first bubbled for 20 min with a mixture of 5 % CO_2 and the rest N_2 to remove all the dissolved O_2. The cultures were then immediately transferred into an incubator with a humidified hypoxic atmosphere containing 5% CO_2, 1 % O_2 in N_2, maintained at 37 °C. After two hours, the OGD in the cultures was terminated by re-supplying the glucose-containing DMEM and transferring them back into an incubator with a normal atmosphere containing 5 % CO_2 in air.

For assessing the mitochondrial depolarization, the control and OGD-subjected cultures were incubated with 100 nM tetramethylrhodamine methylester (TMRM, Molecular Probes, Leiden, Netherlands) at 37 °C for 20-30 min. TMRM was added at time after the OGD termination. For imaging the TMRM fluorescence, excitation was set at 543 nm and

emission was filtered at 570 nm long-pass and the filtered fluorescence light was recorded by photomultipliers. Within one set of experiments, gain and offset of the imaging program were kept constant. Very low laser intensity was used to avoid the photo activation of the dye.

2.3 Patch clamp of the mtPTP

To test the direct effect of melatonin on the mtPTP, we studied single-channel currents through the mtPTP by means of the patch-clamp techniques with mitoplasts, prepared from isolated liver mitochondria, applying different solutions by a flow system.

2.3.1 Preparation of mitoplasts

Liver of male Sprague-Dawley rats were cut in small pieces, homogenized by means of a teflon-pistle and centrifuged for 5 min at 600×g. The resulting supernatant was centrifuged again for 4 min at 5100×g. The pellet obtained was resuspended in an isolation medium containing 250 mM sucrose, 1mM K-EDTA (pH 7.4) and centrifuged for 10 min at 12300 × g. The final pellet containing the mitochondria was resuspended in storage medium and stored on ice for a maximum of 36 h. Mitoplasts were prepared by a hypo-osmotic treatment with the hypotonic buffer containing, 5 mM potassium-HEPES, 0.2 mM $CaCl_2$ (pH 7.2). After one-minute incubation at room temperature, the isotonicity was restored by addition of hypertonic medium: 750 mM KCl, 80 mM K-HEPES, 0.2 $CaCl_2$ mM (pH 7.2).

2.3.2 Electrophysiology

For patch-clamp experiments borosilicate glass pipettes (Clark, Pangbourne, UK) were polished to yield resistances of 12-17 MΩ. Free-floating mitoplasts were approached by the pipette using an electrically driven micromanipulator. The mitoplasts were moved to their final position at the pipette tip by gentle suction. Gigaseals of about 1.5 GΩ were formed spontaneously or by additional suction. Experiments were done in the mitoplast-attached mode. Currents were recorded by an L/M-EPC-7 amplifier (HEKA electronics, Lambrecht, Germany). The currents were low-pass filtered by a 4-pole Bessel filter at a corner frequency of 0.5 kHz. Data were recorded at a sample frequency of 2.5 kHz by means of the pClamp software (Axon instruments, Foster City, CA) which was also used

for processing of the data. Melatonin in different concentrations (0.25, 0.8, 1, 10, 100 μM) was added through the glass capillaries of a peristaltic-pump driven flow system. Potentials given are measured at the inner side of the membrane. Inward currents are always depicted downwards in the traces. The probability that the channel is in an open state (Po) was determined by an all points analysis according to the following equation:

$$Po = \frac{(A1 * B1) + (A2 * B2) + ... + (An * Bn)}{Bmax\ (A0 + A1 + A2 + ... + An)}$$

where Po is weighted by the different amplitudes of the sub-states (Bn), An is the area under the Gaussian curves for the closed state and the different open states [147].

2.4 Statistical analysis

Data are shown as (mean ± SEM). For statistical analysis, one way analysis of variance (ANOVA) was applied followed by Dunnett's Multiple Comparison test. For the results obtained with NMDA induced $[Ca^{2+}]_c$ rise, data were collapsed at every 100 s time point after onset of NMDA application. These data were then treated with two-way ANOVA followed by Tukey's-t-test. $p< 0.05$ was considered to be statistically significant.

2.5 EXPERIMENTAL DESIGN

2.5.1 Direct inhibition of the mitochondrial permeability transition pore: a possible mechanism responsible for anti-apoptotic effects of melatonin

2.5.1.1 Assessment of the effect of melatonin on NMDA-induced intracellular Ca^{2+} alterations by fluo-4 imaging

For the assessment of NMDA-induced intracellular Ca^{2+} changes by fluo-4 imaging, primary neuronal cultures were divided into different groups. In one group, NMDA treatment was started at 100 sec after the start of image acquisition. NMDA dissolved in HBSS was infused continuously for the whole of the experiment. In other two groups of cultures, either melatonin or CsA were continuously infused along with NMDA at 20 s after the start of NMDA application (Scheme 1).

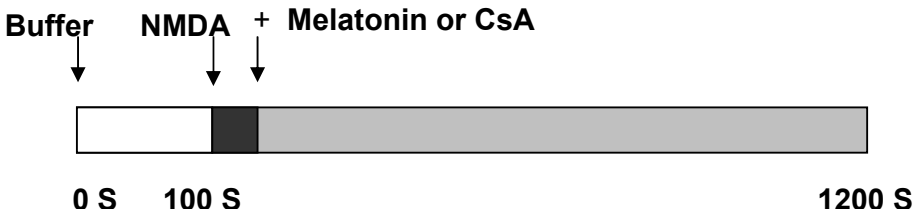

Scheme 1: Protocol for Ca^{2+} imaging. After mounting the Fluo-4 loaded culture on the microscopic stage, the culture was perfused for 0-100 sec with buffer alone. At 100 s continuous infusion of NMDA was started. In other subsets of experiments, either melatonin or CsA was infused at 20 s after NMDA infusion. The experiment was run for a total of 1200 s.

2.5.1.2 Assessment of the effect of melatonin on OGD and mitochondrial depolarisation

In order to access the effect of melatonin on mitochondrial depolarization in oxygen-glucose deprived neurons, the cultures were divided into following groups.

First group: cultures were incubated with TMRM alone and no OGD was subjected. Vehicle 10 % alcohol 4 µl were also added to the culture. This group served as control for other OGD-subjected cultures.

Second group: OGD was subjected for three hours followed by reperfusion. Here again vehicle 10% alcohol (4 µl) was applied.

Third group: melatonin was added and the cultures were subjected to the OGD protocol.

Fourth group: only melatonin was added and no OGD was subjected to the cultures.

Fifth group: CsA (2 µl) was added and the cultures were subjected to the OGD protocol (scheme 2)

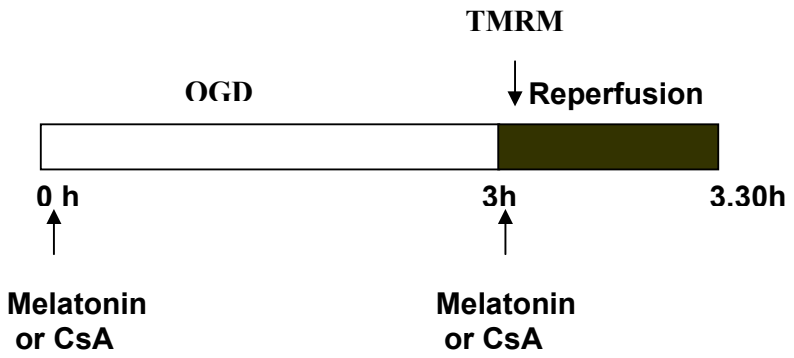

Scheme 2: Protocol for ODG experiments: Melatonin or CsA was treated in the cultures at 0 h of OGD. At 3 h OGD was terminated and melatonin or CsA was treated again. TMRM was loaded into the cultures shortly after the OGD termination. After 30 min reperfusion, cultures were analysed for mitochondrial TMRM uptake, using confocal Zeiss Microscope.

2.5.1.3 Assessment of neuroprotective and antiapoptotic effects of melatonin

To test the antiapoptotic and neuroprotective effects of melatonin in the rat middle cerebral artery occlusion (MCAO), the animals were kept under a 12 h /12 h light/dark cycle and were given free access to food and water. The rats were randomly divided into four treatment groups: “Sham + Vehicle” (injection of vehicle, no occlusion), “Sham + Mel” (rats treated with melatonin only and no occlusion was performed), “MCAO + Vehicle” (MCAO was performed and vehicle was given in place of the drug), and “MCAO + Mel ” (MCAO was applied and the animals were treated with melatonin). In order to make the in-vivo ischemia conditions more close to the clinical situation, MCAO occlusion with intraluminal suture method was used. The MCA was occluded for 2 h followed by reperfusion. For evaluation of neurological deficits, animals were evaluated 24 h after reperfusion for neurological function tests, the infarct volume was evaluated 3 days after reperfusion. Subsets of animals were sacrificed at 4 h and 24 h of reperfusion for the assessment of the cytosolic changes in different apoptotic, Mn-SOD, glutathione peroxidase activity and cell death markers.

2.5.1.4 Melatonin *in-vivo* treatment

In order prepare melatonin solution for *in-vivo* treatment, the drug was dissolved in 10 % alcohol and was injected intraperitoneally (i.p) twice into the rats; at the time of occlusion and at the time of reperfusion. The drug was first dissolved in 100 µl of absolute alcohol and then diluted with normal saline to get a final concentration of 10 % alcohol. Each animal was injected a volume of 1ml / kg of body weight.

2.5.2 Oxyresveratrol (trans-2, 3', 4, 5'-tetrahydroxystilbene) is neuroprotective and inhibits the apoptotic cell death in transient cerebral ischemia

2.5.2.1 Assessment for neuroprotective effects of Oxyresveratrol

For this purpose, the animals were randomly divided into 10 treatment groups (n =10 for each group): "Sham + Vehicle" (sham-operated animal without MCAO and treatment with vehicle only) "Sham + OXY 2" (sham-operated animals, treated with 2 mg OXY), "Sham + OXY 10" (sham-operated animals, treated with 10 mg OXY), "Sham + OXY 20" (sham-operated animals, treated with 20 mg OXY), "Sham + OXY 30" (sham-operated animals, treated with 30 mg OXY), "MCAO + Vehicle" (animals with MCAO and vehicle treatment), "MCAO + OXY 2" (animals with MCAO and 2 mg / kg OXY treatment), "MCAO + OXY 10" (animals with MCAO and 10 mg / kg OXY treatment), "MCAO + OXY 20" (animals with MCAO and 20 mg / kg OXY treatment) and "MCAO + OXY 30" (animals with MCAO and 30 mg / kg OXY treatment).

For evaluation of neurological deficits, animals were evaluated 24 h after reperfusion for neurological function tests, the infarct volume was evaluated 3 days after reperfusion, in a similar way as that of melatonin-treated rats. Subsets of animals were sacrificed at 4 h and 24 h of reperfusion for the assessment of the cytosolic changes in different apoptotic and cell death markers.

2.5.2.2 Oxyresveratrol preparation and treatment

OXY was prepared from mulberry wood as described previously [131]. The purity of the compound was confirmed by TLC, HPLC, and its melting point (mp = 199 – 200 ^{o}C, mp $_{Lit.}$= 201 ^{o}C [148]. The ^{1}H- and ^{13}C NMR-spectral data (UV spectrum: λ_{max} = 328 nm, $\log_{\varepsilon}$ = 4.329) of the purified OXY were consistent with that of the literature [149, 150].

OXY (30, 20, 10 and 2 mg / kg body weight in a total volume of 1 ml in 30 % alcohol) or equal volumes of vehicle were administered intraperitoneally (i.p.) in animals twice: at the time of occlusion and at the time of reperfusion.

3. RESULTS

3.1 Direct inhibition of the mitochondrial permeability transition pore: a possible mechanism responsible for anti-apoptotic effects of melatonin in transient brain ischemia

3.1.1 Melatonin reduced the sustained $[Ca^{2+}]_c$ increase in primary neuronal cultures exposed to NMDA

We first studied if melatonin modulates the NMDA-induced $[Ca^{2+}]_c$ rises as measured by fluo-4 confocal imaging in mouse striatal neurons. Upon stimulation of striatal neurons with 200 μM NMDA, we observed a fast initial increase in the fluo-4 fluorescence from a baseline intensity of 103.4 ± 4.3 (average of single cell arbitrary intensity values ± SEM, n=5 cultures) to a level of 282.3 ± 22.5 immediately after exposure to NMDA (Fig. 1). The increased fluorescence, indicating an increase in $[Ca^{2+}]_c$ did not return to the baseline level but remained at a sustained plateau level for the whole experiment. After 18 min of NMDA application, the fluorescence was still high at 284.3 ± 16.2.

When cyclosporine (CsA, 2 μM) was added to the NMDA-containing superfusion solution, the neurons exhibited again a fast initial increase in the fluorescence, peaking at similar levels (297.3 ± 7.2, n=5 cultures). However, the fluo-4 fluorescence did not remain at the plateau levels with CsA treatment, instead started to decline (Fig. 1). At 5 min of CsA + NMDA application a significant decrease in the NMDA-induced sustained fluorescence was observed (207.7 ± 15.2, $p < 0.05$) and at 18 min of CsA application the values declined to 188.8 ± 23.0 ($p < 0.05$). When melatonin (100 μM) was added to the NMDA-containing superfusion solution, the fluorescence plateau started to decline again in a similar pattern as seen with CsA (Fig. 1). At 5 min of melatonin + NMDA application the fluorescence values significantly decreased from 281.9 ± 12.6 to 230.3 ± 14.7 ($p < 0.05$) and at 18 min of melatonin application to 181.5 ± 11.9 ($p < 0.05$).

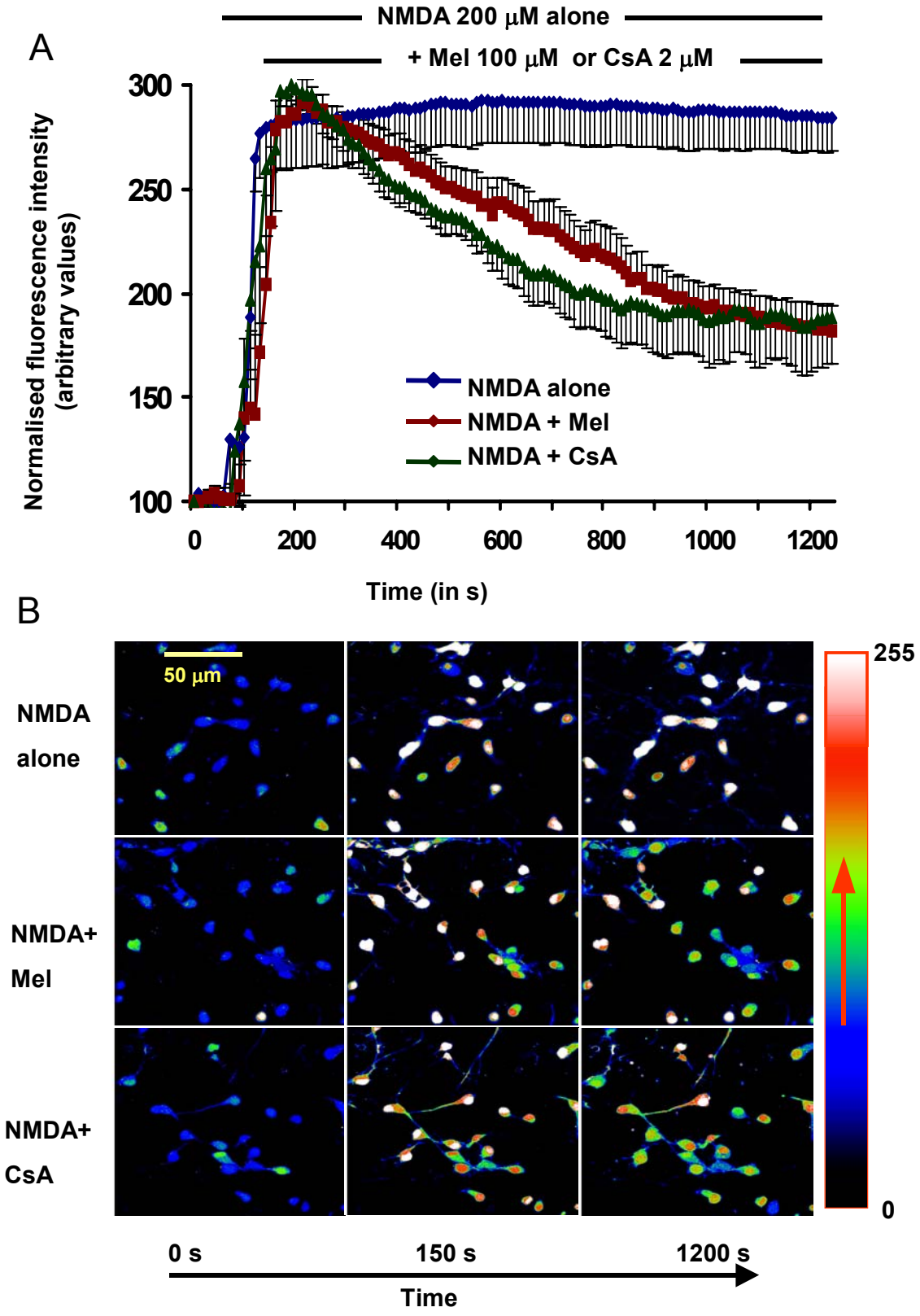
A
NMDA 200 μM alone
+ Mel 100 μM or CsA 2 μM
Normalised fluorescence intensity (arbitrary values)
300
250
200
150
100
0
200
400
600
800
1000
1200
Time (in s)
NMDA alone
NMDA + Mel
NMDA + CsA
B
50 μm
NMDA alone
NMDA+ Mel
NMDA+ CsA
255
0
0 s
150 s
1200 s
Time

Fig. 1: Melatonin decreases NMDA-induced intracellular calcium levels:

Neuronal cultures were loaded with the Ca^{2+}-sensitive fluorochrome fluo-4 and time series of confocal images were recorded to monitor the fluorescence intensities. NMDA was applied alone **(**200 μM, blue line) and or together with CsA (2 μM, green line) or melatonin (100 μM, red line). The black lines above the graph indicate the duration of the treatments.

A : Depicted are the average fluorescence intensity traces of the different treatment groups reflecting the intracellular Ca^{2+} levels. The traces were obtained by analysing the average pixel fluorescence intensity within boxes drawn over single cell somata for each image of the time series. NMDA alone shows a rise in $[Ca^{2+}]_c$ in neurons that sustained at a plateau level throughout the continuous NMDA application. Both, melatonin and CsA decreased the sustained rise in $[Ca^{2+}]_c$ in the NMDA-stimulated neurons. Normalized data are expressed as mean ± SEM, n= 5 cultures for each group.

B: Representative images of the fluo-4-loaded cultures. The left column depicts the baseline fluorescence before the NMDA application, the two other columns show the elevated fluorescence during the NMDA-exposure.

The upper row (NMDA alone) shows the sustained rise in $[Ca^{2+}]_c$ after NMDA application. The middle row (NMDA + Mel) indicates that although these neurons displayed an initial high $[Ca^{2+}]_c$ level after the NMDA exposure onset, the fluorescence decreased in the presence of melatonin. The lower panel of images shows a similar effect of CsA on the NMDA-induced $[Ca^{2+}]_c$ level as seen with melatonin.

3.1.2 Melatonin inhibited the mtPTP

We investigated if melatonin has a direct inhibitory effect on the mtPTP. For that purpose, we recorded the mtPTP channel currents from patches of the inner mitochondrial membrane. The recordings displayed a characteristic activity of the mtPTP with an extremely large single channel conductance of more than 1 nS and a large variety of sub-conductance states that could all be reversibly blocked by 1 μM CsA, (Fig. 2A) as described before [147]. Melatonin inhibited the P_o of mtPTP (Fig. 2C) in a dose dependent manner ranging from 100 μM to 200 nM. The respective concentration response relation is shown in Fig 3C. The best fit by means of the Hill equation was calculated with an IC_{50} of 0.8 μM and a Hill coefficient of 1. A maximum decrease in the P_o to only 80% reflects the fact that the effect of melatonin even at higher concentration is gradual and as the initial records also contribute to the mean P_o, the mean values do not decline to zero, instead saturate at 80% (P_o / P_o max = 0.2). This effect was reversible upon washout in the control solution (Fig. 2B, 4th trace).

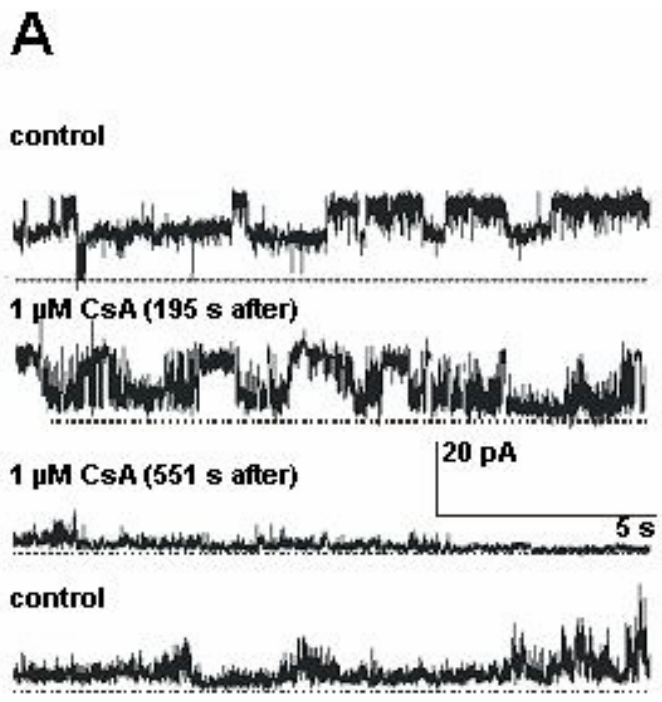

Fig. 2: Melatonin inhibits the mtPTP currents at single channel level:

A: Representative traces of mtPTP activity (control, 1st trace), with CsA application (2nd and 3rd trace) and after switching back to control solution (4th trace).

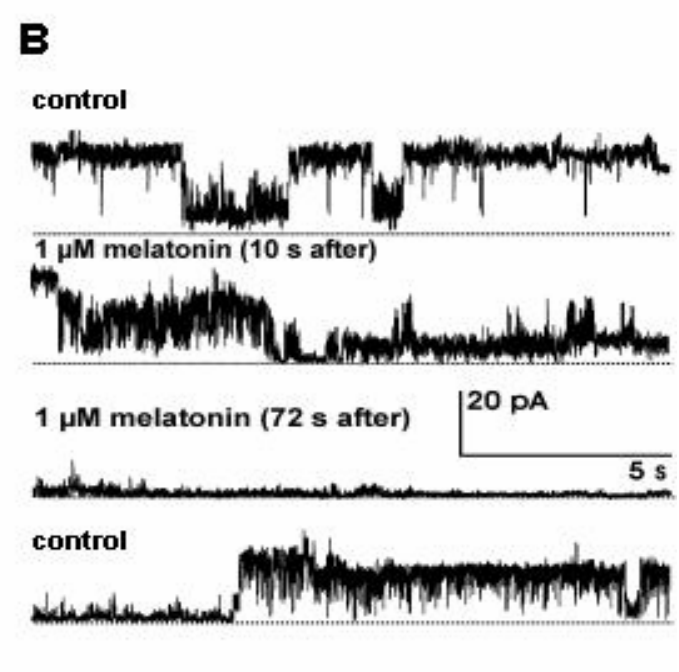
B
control
1 μM melatonin (10 s after)
1 μM melatonin (72 s after)
20 pA
5 s
control

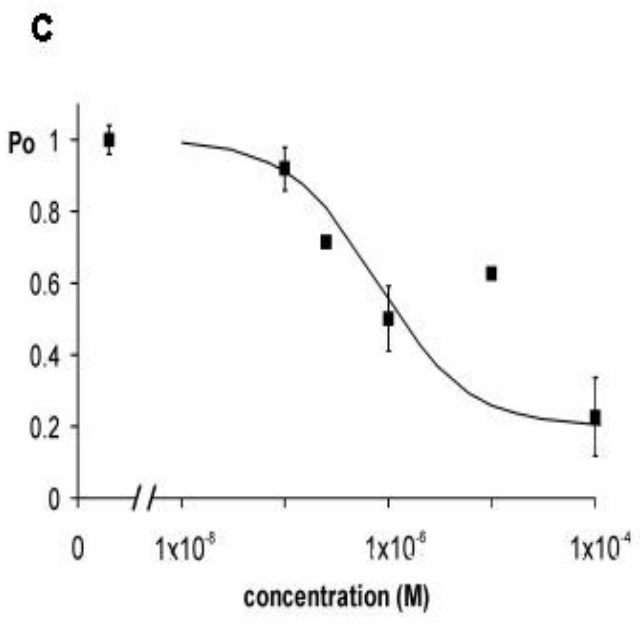
C
Po
1
0.8
0.6
0.4
0.2
0
0
1x10-8
1x10-6
1x10-4
concentration (M)

B: Effect of melatonin on single channel currents recorded from the mtPTP of the mitoplast membrane:
Shown are the representative traces of mtPTP activity with a representative 1 μM melatonin application. The base line mtPTP activity (control, 1st trace) was blocked by 1μM Melatonin (2nd and 3rd trace, at 10 s and 72 s, respectively, after switching to melatonin) which was reversible (4th trace, after switching to control). Dotted lines give zero-current level. Holding potential (E_h) +20 mV.

C: Concentration-response curve for the normalized open propability (Po) under the influence of melatonin at E_h = +20 mV:
Po was estimated by all-point analysis of the single channel data in 1 min segments from each experiment, starting one minute after the addition of melatonin. Mean Po were calculated from 2 independent experiments at each concentration. Data are shown as mean ± SEM and the curve was calculated by means of the Hill equation (Hill coefficient: 1) with a half-maximum P_o (IC_{50}) at 0.8 μM.

3.1.3 Melatonin prevented mitochondrial depolarisation after OGD in primary neuronal cultures

We used the potentiometric fluorescent dye TMRM to monitor its uptake in OGD-subjected mouse striatal neurons in the presence or absence of CsA or melatonin as a measure for the integrity of the $\Delta\psi_m$. Fluorescence images of TMRM-incubated cultures, obtained after 3 h of OGD and 30 min glucose-oxygen resupply, showed only little TMRM fluorescence in mitochondria-like structures, an indication that the mitochondria were largely depolarised after the insult (Fig 3b). The few structures that exhibited TMRM fluorescence displayed an unusual round short shape whereas the mitochondria-like structures in control cultures that did not undergo the OGD procedure showed an intensive fluorescence (Fig. 3a). When the OGD-subjected cultures were additionally treated with 2 μM CsA the loss of TMRM-labelled mitochondria-like structures was partially reversed (Fig 3e). Similarly, a treatment with 100 μM melatonin prevented the loss of TMRM uptake due to OGD. The mitochondrial shape was less disrupted in these cultures (Fig. 3c). Melatonin or CsA *per se* did not alter the TMRM uptake into the neurons that were not subjected to OGD (Fig. 3d). Furthermore we tested the TMRM-uptake into the mitochondria in control cultures that were treated with Verapamil (5 μM) 5 min before

TMRM incubation to inhibit the multi drug resistance pump (MDR). We found that the TMRM-uptake in verapamil treated cultures was not different from that of control cultures, treated with either vehicle, melatonin or CsA (Fig. 4).

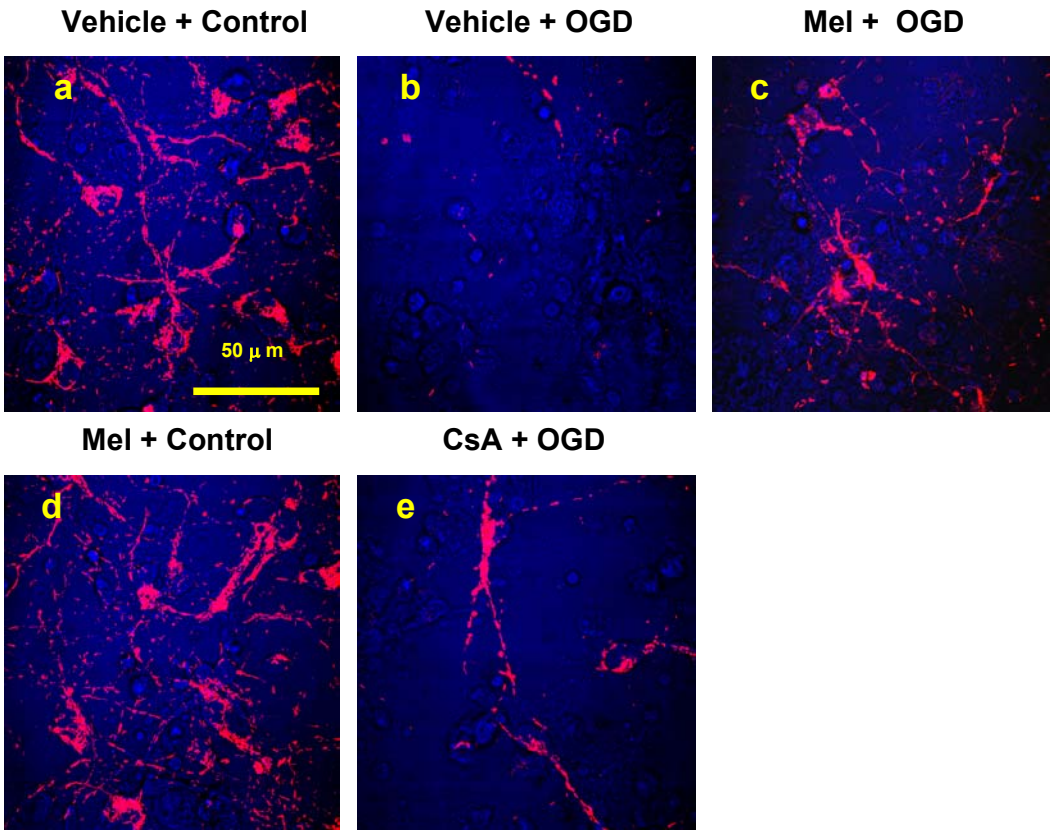

Fig. 3: Melatonin preserves the rate of TMRM uptake after OGD:

Representative pictures showing an overlay of a phase contrast image and an image of the TMRM fluorescence. Red colour shows the TMRM-loaded mitochondria, indicating an intact $\Delta\Psi_m$. The images were obtained after the cultures were subjected to 3 hrs OGD followed by 30 min oxygen-glucose resupply. TMRM was added to the culture medium at the time of oxygen-glucose resupply.

(a) shows a control culture with strongly stained mitochondria-like structures. In (**b**) an OGD-treated culture is shown that has almost completely lost the ability to take up TMRM into the mitochondria indicating a loss of $\Delta\Psi_m$. OGD-subjected cultures (**c**) that contained melatonin (100 µM) in the medium, in contrast, retained the capacity to load TMRM. Melatonin alone (**d**) did not alter the TMRM uptake in control cultures. Analoguous to melatonin, a treatment with 2 µM CsA (**e**) also prevented the loss of $\Delta\Psi_m$ as indicated by the mitochondrial uptake of TMRM in some cells.

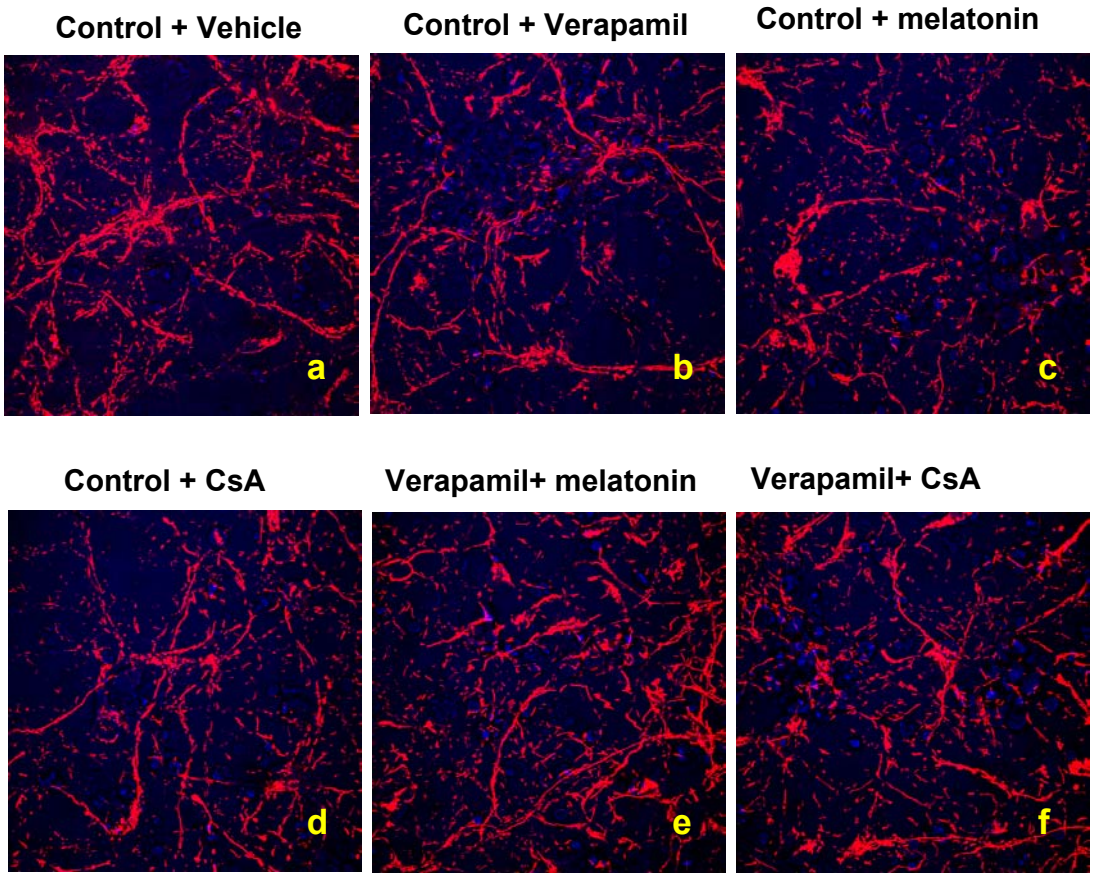

Fig. 4: TMRM uptake in control cultures, **(a)** treated with either vehicle, **(b)** verapamil (5μM), **(c)** melatonin (100 μM), **(d)** CsA (2 μM) **(e)** verapamil 5 μM + melatonin 100 μM or **(f)** verapamil 5 μM + CsA 2 μM . In vehicle-control culture (**a**) well defined mitochondrial-TMRM uptake is seen. Control cultures (**b**) treated with verapamil (5 μM), incubated 5 min before TMRM application, showed a similar TMRM uptake as seen in vehicle-control cultures **(a).** There is no difference in TMRM-staining between verapamil-treated cultures **(b)** or melatonin-treated cultures **(c)** or CsA-treated cultures **(d)** and vehicle control cultures **(a).** Also in cultures, where verapamil was treated in combination with melatonin **(e)** or in combination with CsA **(f),** no difference is observed in TMRM staining as compared to vehicle-control cultures **(a)**.

3.1.4 Anti-apoptotic effects of melatonin in the MCAO model of cerebral ischemia

3.1.4.1 Melatonin prevented the release of cyt c release from mitochondria

We explored the effect of melatonin treatment on the cytosolic cyt c immunoreactivity in brain sections of the infarct area in MCAO rats, using immunohistochemistry. MCAO followed by reperfusion in the "MCAO + Vehicle" group caused a pronounced increase in the cytosolic cyt c immunoreactivity at 4 h as well as 24 h after the reperfusion (Fig. 5A). At 4 h, the cytosol was strongly stained for cyt c immunoreactivity. At 24 h after reperfusion, the cyt c immunoreactivity extended even to the intercellular space (Fig. 5A) indicating massive degeneration of the cells and shedding off the intracellular contents into the intercellular spaces. In contrast, the "Sham + Vehicle" rats showed a profile cyt c staining at both 4 h as well as 24 h (Fig. 5A) that was indicative of intact mitochondria. When MCAO-subjected animals were treated with melatonin "MCAO + Mel", the cytosolic cyt c immunostaining as well as the intercellular cyt c staining signals decreased both at 4 has well as 24 h (Fig. 5A).

3.1.4.2 Melatonin prevented caspase-3 activation

At 4 h of occlusion, sections of "MCAO + Vehicle" rats showed a massive activation of caspase-3 in the ischemic cortex as compared to the "Sham + Vehicle" rats (Fig. 5B) that was still detectable at 24 h after reperfusion but not localised in well-defined cellular compartments (Fig. 5B). Upon melatonin treatment, the caspase-3 activation was drastically reduced in "MCAO + Mel" rats both at 4 h and 24 h (Fig. 5B). No changes in caspase-3 staining were observed in "Sham + Mel" rats when compared to "Sham + Vehicle" rats.

3.1.4.3 Melatonin reduced apoptotic DNA fragmentation

In "MCAO + Vehicle" rats, the Apostain label was observed in the nuclei of a large cell population. Such Apostain-positive cells showed a characteristic morphology of apoptotic

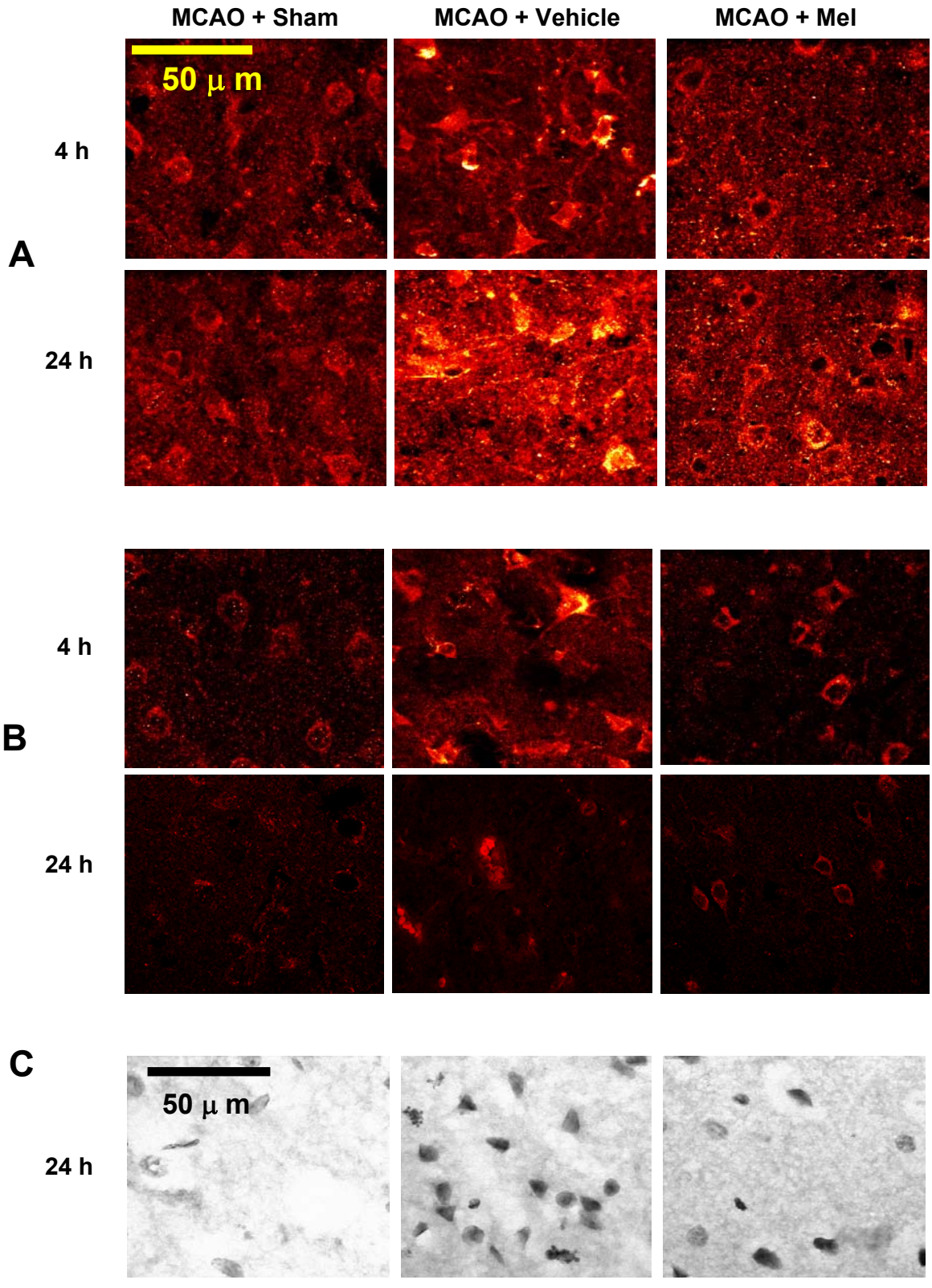
MCAO + Sham
MCAO + Vehicle
MCAO + Mel
50 μ m
4 h
A
24 h
4 h
B
24 h
C
50 μ m
24 h

cells with shrunken structures. The number of Apostain-positive cells were reduced by melatonin in "MCAO + Mel" rats (Fig. 5C), showing an anti-apoptotic effect of melatonin.

Fig. 5: Melatonin inhibited the apoptotic cell death in MCAO rats:

A: Cytosolic cyt c immunoreactivity is decreased in MCAO brain tissue upon melatonin treatment:
Representative pictures of the cyt c immunostaining in the MCA-supplied cortex obtained at 4 h (upper panel) or 24 h (lower panel). No specific cytosolic immunostaining is seen in the "Sham + Vehicle" rats, both at 4 h and 24 h. Characteristic cyt c labelling in the cytosol of cells is observed after 4 h and 24 h in the "MCAO + Vehicle" rats. After 24 h the staining is seen in the intercellular spaces indicating the presence of cell debris. Melatonin treatment greatly reduces the cytosolic cyt c immunostaining in "MCAO + Mel" rats both at 4 h as well as 24 h.

B: The MCAO induced caspase-3 immunoreactivity is reduced by melatonin:
Corresponding caspase-3 immunofluorescence of the MCA-supplied cortex in the sections adjacent to those seen in A. No activation of caspase-3 is seen in "Sham + Vehicle" rats while in vehicle treated MCAO rats, most of the cells show an increased caspase-3 immunostaining at 4 h. At 24 h an increased and patchy caspase-3 immunostaining is seen in "MCAO + Vehicle" rats. Melatonin treatment decreases the caspase-3 activation both at 4 h and 24 h after ischemia "MCAO + Mel" rats.

C: Melatonin protects against MCAO-induced DNA fragmentation:
Images of Apostain-labelled cortices, indicating the presence of apoptotic ssDNA. In "Sham + Vehicle" rats, no staining is observed while in the "MCAO + Vehicle" rats, most of the cells are Apostain-labelled. The darkly stained cells are shrunken and have a characteristic apoptotic-like appearance. Melatonin decreased the number of apopstain-positive cells in "MCAO + Mel" rats.

3.1.5 Melatonin reduced the MCAO-induced brain damage

3.1.5.1 Decrease in the infarct volume

TTC staining of brain slices obtained from "MCAO + Vehicle" rats showed reproducible and readily detectable lesions in the areas that are supplied by MCA, at 3 days after the reperfusion (Fig. 6A1). The lesions were present both in the lateral striatum and the overlying cortex. Melatonin, when given at the onset of occlusion and reperfusion in "MCAO + Mel" rats, reduced significantly the infarct volume to 147.0 ± 10.4 mm^3, ($p<0.05$, n=10) as compared to "MCAO + Vehicle" rats (290.0 ± 13.5 mm^3, n=10, Fig. 6A2).

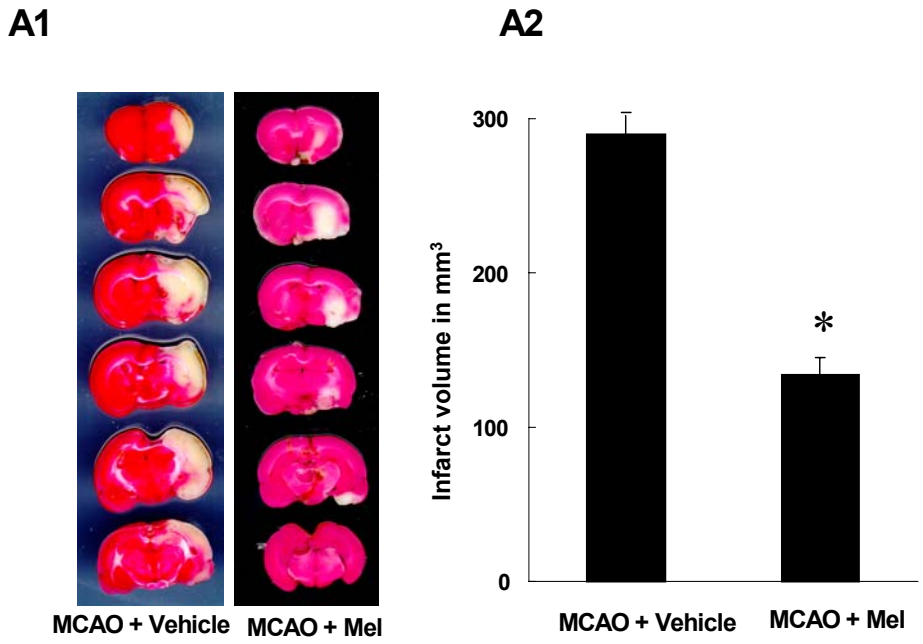

Fig. 6: Melatonin reduces the infarct volume:

A1: TTC-stained coronal sections from representative animals that received either vehicle (10% ethanol) or melatonin (10mg/kg, i.p.) both at the time of occlusion as well as at the time of reperfusion. The animals were euthanised 3 days after occlusion. Infarcts are observed as pale regions involving striatum and overlying cortex. Note that the infarct area in the melatonin-treated animal is substantially reduced.

A2: Statistical analysis of infarct volume:

Reproducible infarct volumes are observed in the "MCAO + Vehicle" rats subjected to 2 h occlusion followed by 3 days reperfusion. Melatonin significantly reduced the infarct volume in "MCAO + Mel" (*$p<0.05$, $n=10$). Data are expressed as mm^3 and represent mean ± SEM.

3.1.5.2 Prevention of the loss of MAP-2 and NeuN staining in the ischemic tissue

To elucidate at the cellular level, the extent to which neurons are protected in melatonin-treated MCAO rats, we studied the changes in MAP-2 and NeuN immunoreactivity in the cortical infarct area. In the "Sham + Vehicle" rats, the MAP-2 staining was characterised by a uniform strong fluorescence of both dendrites and soma (Fig. 7A). After 24 h of reperfusion, a pronounced loss of MAP-2 staining (Fig. 7A) was observed in the "MCAO + Vehicle" group, whereby some localised beaded pattern of immunoreactive structures remained. After melatonin treatment "MCAO + Mel", the MAP-2 staining was preserved both, in the dendritic arbour and soma in the ischemic cortex of "MCAO + Mel" rats at 24 h after reperfusion (Fig. 7A).

A well defined NeuN staining was observed in "Sham + Vehicle" rats. In contrast, the NeuN-positive cells were almost completely lost from the ischemic cortex in "MCAO + Vehicle" rats at 24 h after the start of reperfusion (Fig. 7A), indicating a massive neuronal degeneration. Melatonin treatment greatly prevented the loss of NeuN-positive cells after 24 h of reperfusion in "MCAO + Mel" rats.

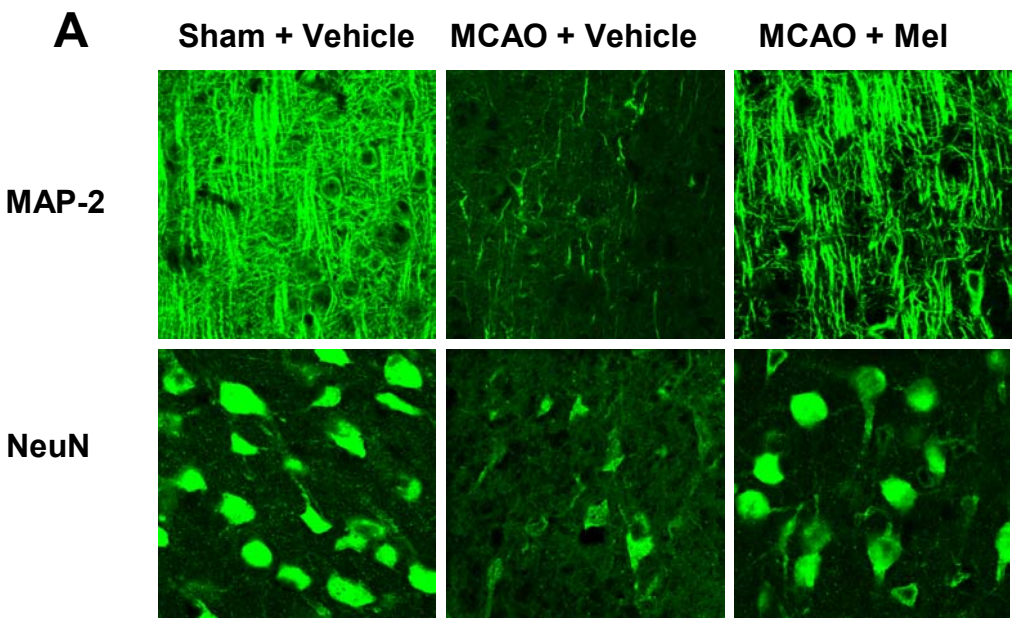

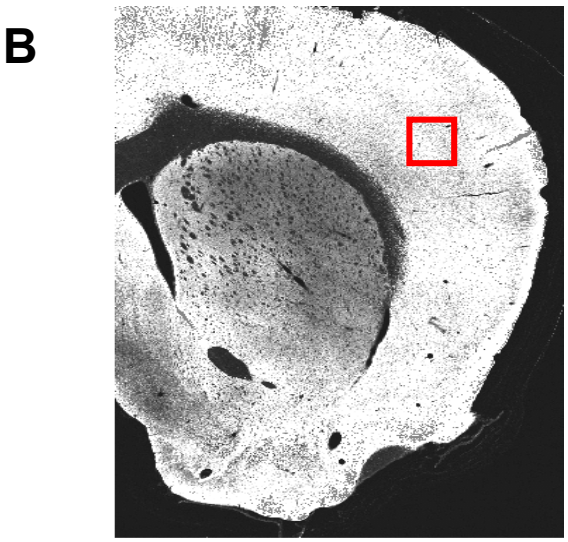

Fig 7A: MAP-2 and NeuN immunostaining:

The upper panel of pictures shows MAP-2 immunostaining in sham-operated , vehicle- treated and melatonin-treated rats, subjected to 2 h occlusion followed by 24 h reperfusion. Neurons in "Sham + Vehicle" rats have an extensive array of branching dendrites and well defined somta stained for MAP-2.

A loss of both, somatic and dendritic MAP-2 labelling is observed in “MCAO + Vehicle” rats at 24 h after reperfusion. Melatonin treatment prevented the loss of MAP-2 staining in “MCAO + Mel” rats.
The lower panel shows NeuN immunostaining of sections from the same groups as shown in the upper panel. In “Sham + Vehicle” rats, a dense pattern of NeuN-positive cells is observed. In the “MCAO + Vehicle” rats, the NeuN-positive cells are almost completely lost at 24 h after reperfusion. Melatonin preserved the NeuN-positive cells in the ischemic tissue of the “MCAO + Mel ” group.

Fig. 7B: Area of analysis:
For microscopic analysis of the different antigens a location within the MCA-supplied cortex was chosen, that consistently showed lesions in the “MCAO + Vehicle” group and was seen to be recovered by drug treatments. Using landmarks such as the shape of the corpus callosum, the anterior commissure and the outer rim of the cortex, this region was identified as the upper lip region of the somatosensory cortex in the coronal sections that were taken approx 0.2 mm anterior to bregma according to the Paxon and Watson Rat Brain stereotaxic atlas [151]. Therefore the observation field, as indicated by the location of the red box in the image, was placed within the coordinates 5-6 mm lateral to midline and 3-4 mm ventrally from the dorsal surface. The placement of the observation field was kept constant to enable comparisons of the immunofluorescence signals between the different treatment groups.

3.2 Oxyresveratrol (trans-2, 3', 4, 5'-tetrahydroxystilbene) is neuroprotective and inhibits the apoptotic cell death in transient cerebral ischemia

3.2.1 Physiological parameters

Table I shows the summary of physiological parameters before and during ischemia. OXY treatment did not produce any change in the blood gases, pH, mean arterial blood pressure, blood glucose and hematocrit.

Table 1: Physiological parameters for different treatment groups

	15 min before ischemia		0 min of ischemia		30 min of ischemia	
Experimental Groups	**MCAO + Vehicle**	**MCAO + OXY 20**	**MCAO + Vehicle**	**MCAO + OXY 20**	**MCAO + Vehicle**	**MCAO + OXY 20**
pH	7.4 ± 0.03	7.4 ± 0.03	7.2 ± 0.2	7.2 ± 0.03	7.3 ± 0.06	7.3 ± 0.03
$^{P}CO_2$ (mm Hg)	34.7 ± 6.1	37.4 ± 5.8	43.7 ± 4.1	42.7 ± 5.2	34.7 ± 6.1	38.7 ± 8.0
$^{P}O_2$ (mm Hg)	208.3 ± 8.8	217 ± 12.2	193.4 ± 10.8	208 ± 6.1	208 ± 8.7	198.3 ± 10.9
HCT (%)	39.0 ± 0.6	39.7 ± 0.7	40 ± 1.5	40.7 ± 0.9	39.7 ± 1.2	38.7 ± 0.03
BGlu (mg/ml)	8.9 ± 0.3	9.2 ± 0.5	8.9 ± 1.2	8.0 ± 1.1	9.1 ± 0.5	9.5 ± 0.5

Hematocrit (Hct); blood glucose (BGlu); mean arterial blood pressure (MABP).

All animals were maintained at 36.5± 0.5°C rectal temperature.

3.2.2 OXY treatment improved the neurological deficits in MCAO rats

Evaluation by both method A and B showed no neurological deficits in “Sham + Vehicle” rats while in the animal-group “MCAO + Vehicle”, the neurological deficits were severe at 24 h after reperfusion. The “MCAO + Vehicle” rats consistently showed circling movements and postural abnormalities besides other neurological signs like less to no spontaneous movements and severe paw flections. OXY treatment (10, 20 and 30 mg / kg dose) significantly ($p < 0.05$) improved the neurological outcome in “MCAO + OXY 10”, “MCAO + OXY 20” and “MCAO + OXY 30” rats as compared to the “MCAO + Vehicle” rats (Fig. 8). In “MCAO + OXY 10”, “MCAO + OXY 20” and “MCAO + OXY 30” animals, less disturbances in posture and no circling movements were observed when compared to the “MCAO + Vehicle” rats. There were no significant differences in the neurological deficits between the animals of “MCAO + OXY 10”, MCAO + OXY 20 and “MCAO + OXY 30” group (Fig. 8). In the SMA test (method B) the rats in the “MCAO + Vehicle” group spend most of the time in the center of the cage with posture curved towards the paretic side while “MCAO + OXY 10”, MCAO + OXY 20 and “MCAO + OXY 30” rats moved around in the cage and explored their environment. By increasing the dose to 30 mg / kg, no further neuroprotection was seen. There were no significant differences in the neurological scoring between OXY-treated (2, 10, 20 and 30 mg dose) and vehicle-treated sham-operated rats. (data shown for 20 mg dose only).

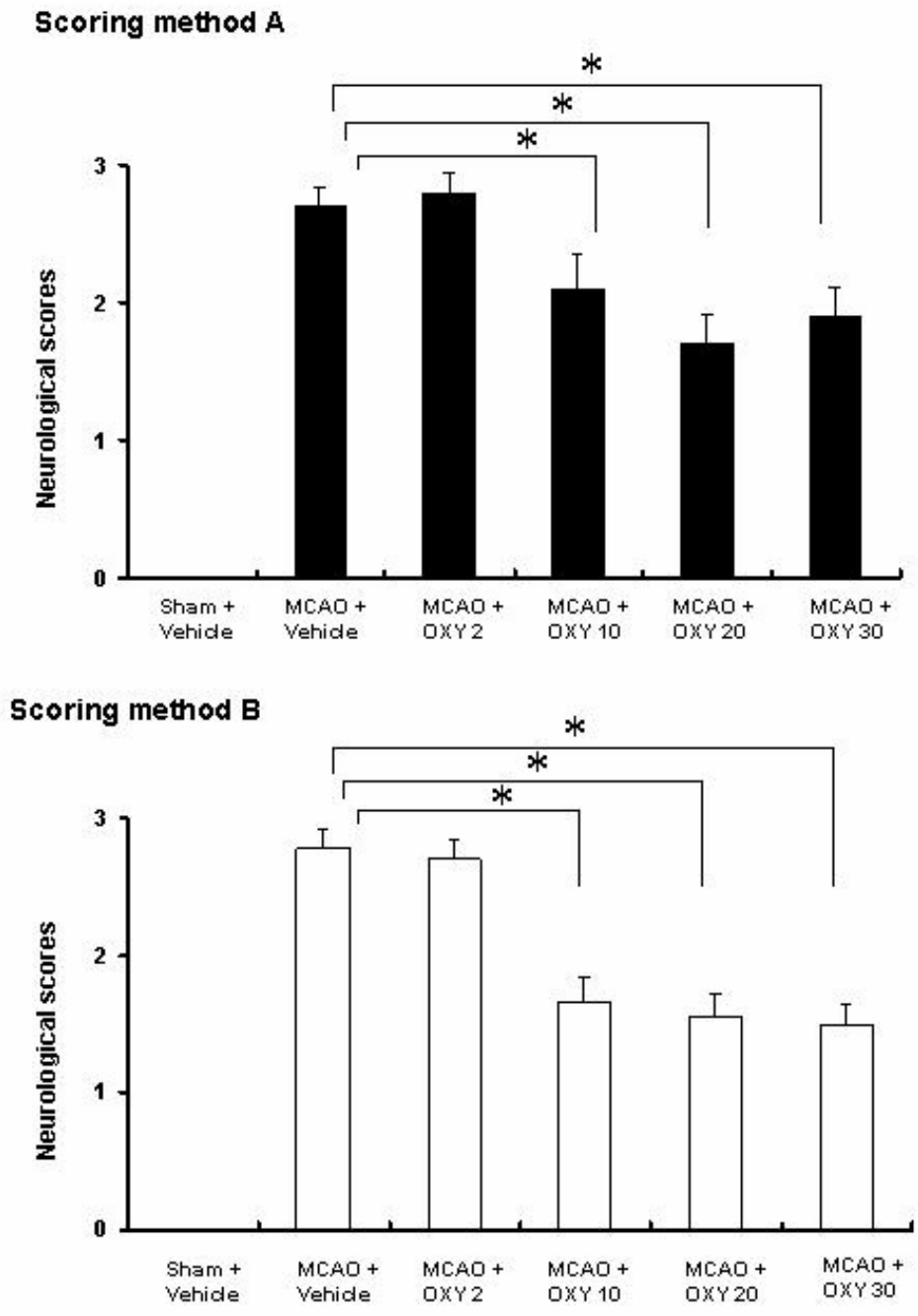

Fig. 8: OXY treatment improved the neurological function in MCAO rats:

Neurological deficits in rats that were subjected to MCAO, measured by scoring methods A and B. "MCAO + Vehicle" rats showed severe neurological deficits 24 after occlusion as compared to "Sham + Vehicle" rats. 10, 20 or 30 but not 2 kg OXY i.p. improved the neurological status significantly ($p < 0.05$). There was no further improvement in the neurological deficits with 30 mg. Data represents mean ± SEM for each group (n =10).

3.2.3 OXY reduced the infarct volume in MCAO rats

TTC staining of brain sections obtained from "Vehicle + MCAO" rats showed reproducible and readily detectable lesions in the areas that are supplied by the MCA at 3 days after the reperfusion (Fig. 9 A). The lesions were present in both the lateral striatum and the overlying cortex. OXY (10 or 20 mg / kg i.p.) reduced significantly the infarct volume to 166.2 ± 12.5 mm^3 and 145.0 ± 11.5 ($p < 0.05$, $n = 8$) respectively, as compared to the "MCAO + Vehicle" group (261.0 ± 18.5 mm^3, $n = 8$, Fig. 9 B). There was no significant difference in the infarct volume between vehicle treated and OXY 2 treated MCAO rats ("MCAO + Vehicle" and "MCAO + OXY 2", respectively). By increasing the dose to 30 mg / kg, no further protection was seen.

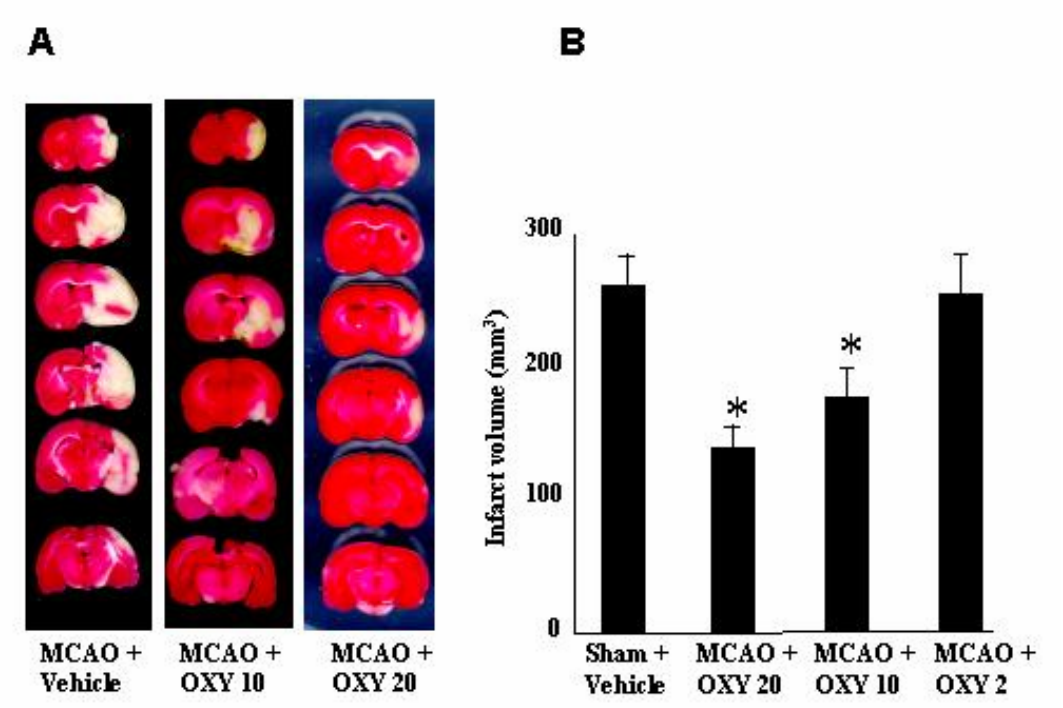

Fig. 9: OXY reduces the infarct volume:

A. TTC-stained coronal sections from representative MCAO-subjected animals that received either vehicle or OXY (10 or 20 mg / kg i.p.) at the time of occlusion and at reperfusion (euthanised 3 days after the experiment). The infarcts, observed as pale regions, are considerably smaller in OXY treated rats when compared to the vehicle-treated animal.

B. Statistical analysis of infarct volume:

Infarct volumes were significantly (*$p < 0.05$) reduced after OXY 20 and Oxy 10 treatment in MCAO rats. There was no significant difference in the infarct volume between OXY 2 and vehicle treated MCAO rats. Data are expressed as mm^3 and represents mean ± SEM (n = 8 in each group).

3.2.4 Histological analysis

Since the 20 mg / kg dose was maximal effective in improving the neurological deficits and in reducing the infarct volume, we used this dose for further evaluation of effects on the apoptotic cascade and for assessing the markers of neuronal degeneration, using immunohistochemical techniques. Microscopic analysis was carried out in the region specified in Fig. 7 B.

3.2.4.1 MAP-2 and NeuN staining in the ischemic tissue

To assess the extent to which neurons are protected in OXY-treated MCAO rats, we studied the changes in MAP-2 and NeuN immunoreactivity in the ischemic cortical area, depicted in Fig. 7 B. In “Sham + Vehicle” group, the MAP-2 staining was characterized by a uniform strong fluorescence of both dendrites and soma (Fig. 10) indicating intact neurons. After 24 h of reperfusion, a pronounced loss of MAP-2 staining (Fig. 10) was observed in the “MCAO + Vehicle” animals, whereby some localized beaded patterns of immunoreactive structures remained. After OXY treatment in “MCAO + OXY 20” rats, the MAP-2 staining was preserved both in the dendritic arbour and the somata of the neurons in the ischemic cortex 24 h after reperfusion (Fig. 10).

A well-defined NeuN staining was observed in “Sham + Vehicle” rats (Fig. 10). In contrast, the NeuN-positive cells were almost completely lost from the ischemic cortex in “MCAO + Vehicle” group at 24 h of reperfusion (Fig. 10), indicating a massive neuronal

degeneration. OXY treatment prevented the loss of NeuN-positive cells after 24 h of reperfusion in "MCAO + OXY 20" rats.

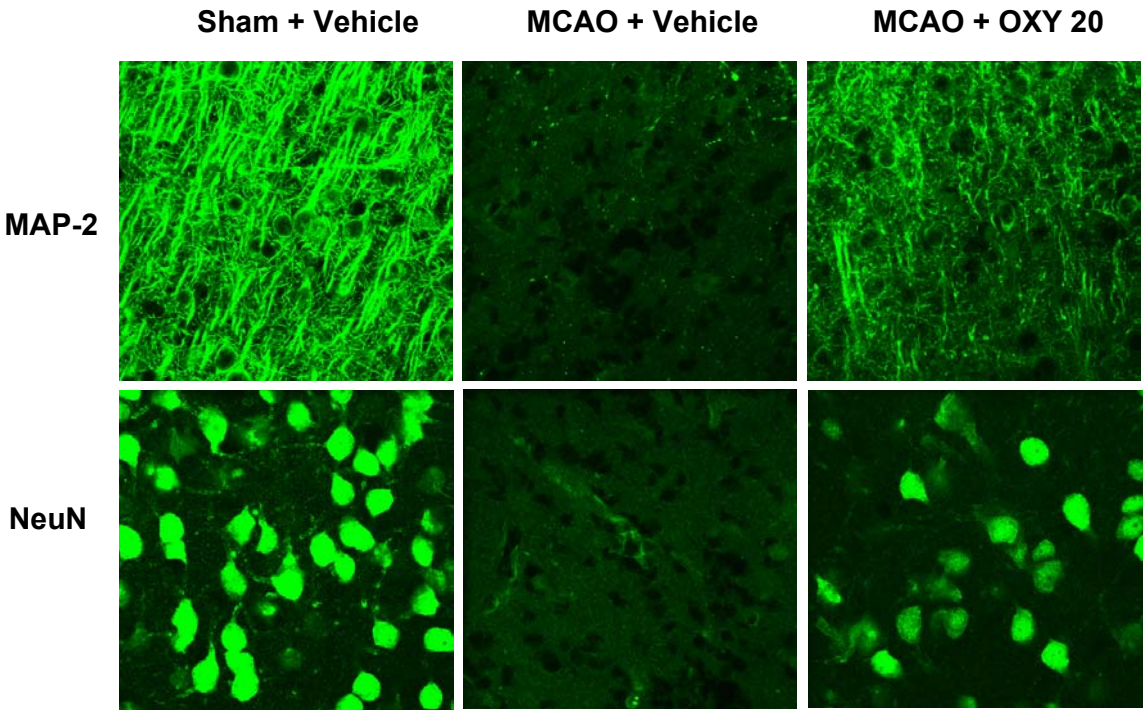

Fig. 10: MAP-2 and NeuN immunostaining:

The upper panel of pictures shows MAP-2 immunostaining in coronal brain sections of different experimental groups. Typical neuronal structures with an extensive array of branching dendrites and well defined somata are seen in "Sham + Vehicle". A loss of both somatic and dendritic MAP-2 labeling is observed in "MCAO + Vehicle" rats at 24 h after reperfusion. OXY treatment prevented largely the loss of MAP-2 staining.

The lower panel shows NeuN immunostaining of sections from the same animals as shown in the upper panel. In "Sham + Vehicle" rats, a dense pattern of NeuN-positive cells is observed. In the "MCAO + Vehicle" rats, NeuN-positive cells are almost completely lost at 24 h after reperfusion. OXY treatment prevented the loss of NeuN-positive cells.

3.2.4.2 OXY prevented cyt c release from mitochondria

MCAO followed by reperfusion in the "MCAO + Vehicle" group caused a pronounced increase in cytosolic cyt c immunoreactivity 4 h as well as 24 h after the reperfusion (Fig. 11 A). At 4 h, the cytosol was strongly stained for cyt c immunoreactivity. 24 h after reperfusion, cyt c immunoreactivity was additionally detected in the extracellular spaces (Fig. 15 A), whereas "Sham + Vehicle" rats showed a cyt c staining pattern at both 4 h as well as 24 h (Fig. 11 A) that was indicative of intact mitochondria. When MCAO-subjected animals were treated with OXY "MCAO + OXY 20", the cytosolic cyt c immunostaining as well as the extracellular cyt c staining signals decreased both at 4 h and 24 h (Fig. 11 A) as compared to "MCAO + Vehicle" animals.

3.2.4.3 OXY prevented caspase-3 activation

At 4 h of reperfusion, sections of "MCAO + Vehicle" animals showed a strong immunoreactivity for caspase-3 in the ischemic cortex as compared to the "Sham + Vehicle" group (Fig. 11 B). An increased caspase-3 immunoreactivity was still detectable at 24 h after reperfusion, however, the caspase-3 immunoreactivity was not only localised in well defined cellular compartments (Fig. 11 B) but was also in cell debris. Upon OXY treatment, the caspase-3 activation was strongly reduced in "MCAO + OXY 20" rats at both the investigated-time points (Fig. 11 B). No changes in caspase-3 staining were observed in "Sham + OXY 20" rats when compared to "Sham + Vehicle" rats.

3.2.4.4 OXY reduced apoptotic DNA fragmentation

In "MCAO + Vehicle" rats, the Apostain-label was observed in the nuclei of a large number of cells. Such Apostain-positive cells showed a characteristic morphology of apoptotic cells with shrunken structures. The number of Apostain-positive cells was reduced in the OXY-treated MCAO "MCAO + OXY 20" rats (Fig11 C) showing an anti-apoptotic effect of OXY.

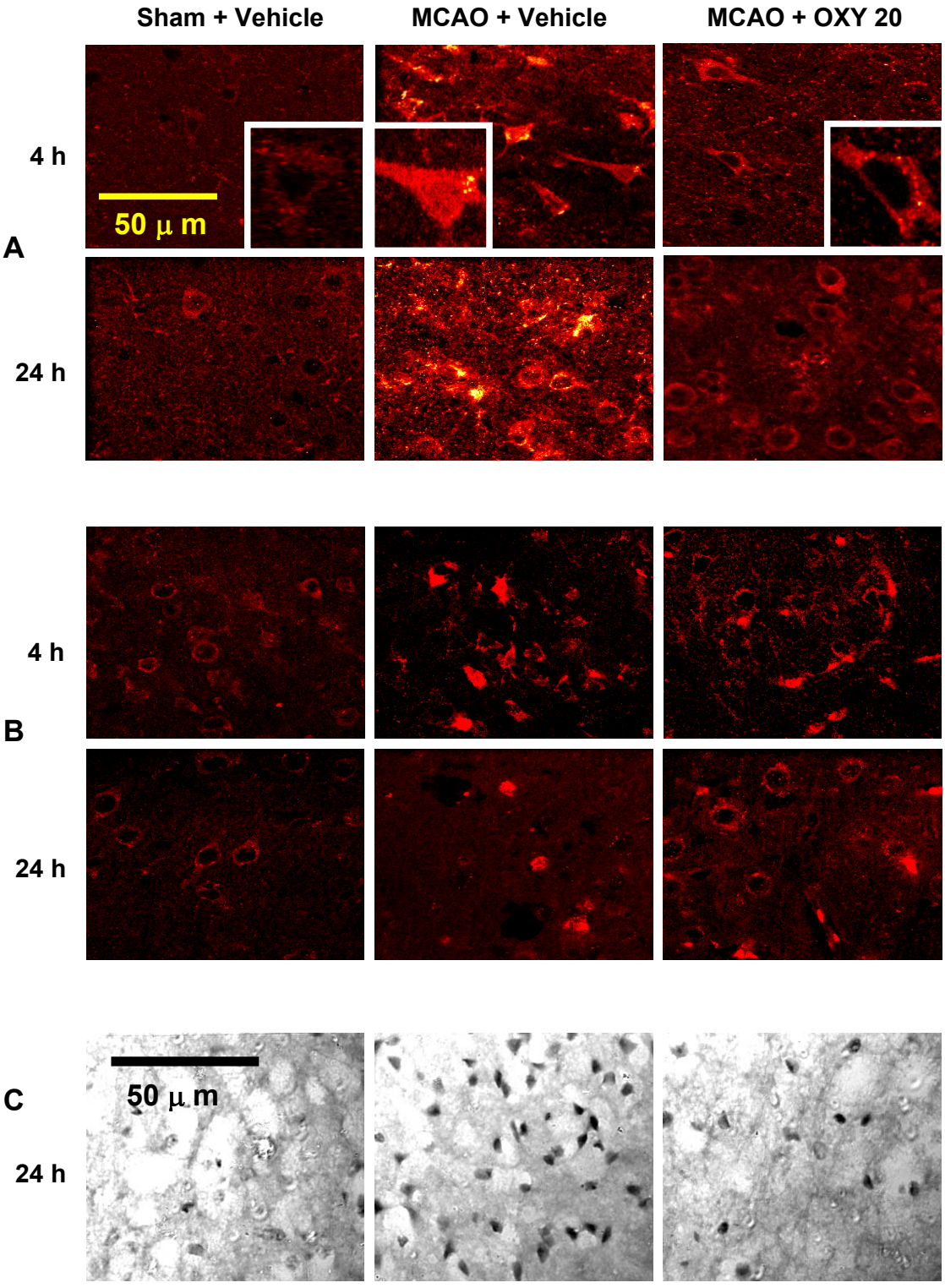
Sham + Vehicle
MCAO + Vehicle
MCAO + OXY 20
4 h
A
50 μ m
24 h
4 h
B
24 h
C
50 μ m
24 h

Fig. 11: OXY treatment inhibited the apoptotic cell death in MCAO rats:

A. Cytosolic cyt c immunoreactivity is decreased in MCAO brain tissue upon OXY treatment:

Representative images of cyt c immunostaining in the MCA-supplied cortex (for location, see Fig. 7B), obtained at 4 h (upper panel) or 24 h (lower panel) after reperfusion. No specific cytosolic immunostaining is seen in the "Sham + Vehicle" rats at 4 h and 24 h. Characteristic cyt c labeling in the cytosol of cells is observed at 4 h and 24 h in "MCAO + Vehicle" rats. 24 h later, the staining is also present in the intercellular space indicating the presence of cell debris. OXY 20 treatment reduces the cytosolic cyt c immunostaining in "MCAO + OXY 20" rats both at 4 h and 24 h after reperfusion. Inserts are showing the magnified views of selective cyt c positive neurons.

B. MCAO-induced caspase-3 immunoreactivity is reduced by OXY:

Caspase-3 immunofluorescence of the MCA-supplied cortex in the sections adjacent to those seen in A. No activation of caspase-3 is seen in "Sham + Vehicle" rats while in "MCAO + Vehicle" rats, most of the cells show an increased caspase-3 immunostaining at 4 h and 24 h after reperfusion. OXY treatment decreased the caspase-3 activation both at 4 h and 24 h after ischemia in "MCAO + Oxy 20" rats.

C. OXY protects against MCAO-induced DNA fragmentation:

Images of Apostain-labeled cortices, indicating the presence of apoptotic ssDNA. In "Sham + Vehicle" rats, no staining is observed while in the "MCAO + Vehicle" rats most of the cells are Apostain positive. The darkly stained cells are shrunken and have a characteristic apoptotic-like appearance. OXY treatment decreased the number of Apostain-positive cells in "MCAO + OXY 20" rats.

4. DISCUSSION

4.1 Direct inhibition of mtPTP by melatonin and its anti-apoptotic effects in cerebral ischemia

We were prompted to consider an action of melatonin on the mtPTP pathway by the initial observation that melatonin decreased the NMDA-induced sustained $[Ca^{2+}]_c$ plateaus. Such elevated $[Ca^{2+}]_c$ during continuous NMDA application is a result of Ca^{2+} influx and internal trafficking of the Ca^{2+} load whereby endoplasmic and mitochondrial Ca^{2+} uptake as well as Ca^{2+} release from these sites plays a role. The mitochondria act as Ca^{2+} buffers by sequestering excess Ca^{2+} from the cytosol. The $[Ca^{2+}]_c$ continues to rise when NMDA receptors are continuously stimulated causing Ca^{2+} uptake into the mitochondria that upon reaching a threshold level leads to mtPTP opening, which in turn produces Ca^{2+}-induced Ca^{2+} release [152]. The mitochondrial permeability transition, allowing the non-selective permeation of ions and solutes through the mitochondrial membrane, is CsA sensitive [105, 153]. Indeed, our experiments, using CsA at a low concentration that is primarily known to block the mtPTP [152], lowered the NMDA-induced $[Ca^{2+}]_c$ levels. This effect indicates the presence of a mtPTP-mediated Ca^{2+} release that contributes to the overall $[Ca^{2+}]_c$ level in our cell culture model.

Melatonin, when used analogous to the CsA treatment, showed in our experiments an almost identical pattern in reducing the NMDA-induced $[Ca^{2+}]_c$ levels as seen with CsA. Such observation would indicate either a direct effect of melatonin on the mtPTP or on mechanisms upstream of mtPTP activation. One of such upstream factors is excessive free radical levels that may also lead to an mtPTP induction. Indeed, we showed earlier that the NMDA-induced $[Ca^{2+}]_c$ rises possess a component that is due to mtPTP activation by NO [146]. Taking in account that melatonin is an excellent radical scavenger and antioxidant [116] one would assume that the observed effect on $[Ca^{2+}]_c$ after NMDA is due to the removal of NO or other reactive oxygen species that are believed to lead to the pathological mtPTP formation [154].

However, we show here that another mechanism, the observed direct inhibition of the mtPTP, is likely to contribute also to this effect. The mtPTP patches obtained from mitoplasts, derived from liver mitochondria showed the characteristic voltage dependence and large conductance of more than 1 nS [147]. The observed blockade of mtPTP currents

by CsA application to the mitochondrial membrane patches together with the earlier shown Ca^{2+}-dependence indicate that the investigated megachannel was indeed the mtPTP. Comparability of mtPTP behavior in mitoplasts with observations made using O_2-measurements or a swelling assay (published as an abstract, Siemen et al., 2002, Restorative Neurology and Neuroscience 20:275-276) make it unlikely that the osmotic shock could have unpredictably altered the behaviour of the mtPTP. As the patches were prepared at high Ca^{2+} concentration mostly fully open mtPTPs were detected at the time of experiment. This comprises an advantage for the patch clamp technique because potentially mtPTP-modulating factors like free radicals, which are effective upstream of the direct interactions with the channel, are excluded. Hence, the observed dose-dependent reduction in the pore currents due to bath application of melatonin is solely due to a direct interaction of melatonin with the channel. Our data show that the efficacy of melatonin in inhibiting the mtPTP is high with an IC_{50} of 0.8 μM. The inhibitory effect started quickly at 10 s after the addition of melatonin to the patch-clamp bath solution and the effect was seen even at very low concentrations (200 nM). In the light of the well known reducing capacity of melatonin one could speculate that a direct action on the mtPTP is possibly a common feature of antioxidants. However, preliminary results in our laboratory using the polyphenolic hydroxystilbene oxyresveratrol show that this antioxidant [155] failed to block mtPTP currents.

Previous studies using various other mtPTP blocking agents show that in pathological conditions such as ischemia, an excessive loading of Ca^{2+} into the mitochondria induces apoptosis by stimulating the release of apoptosis-promoting factors like cyt c, AIF, Smac/DiaBLO and procaspases from the mitochondrial intermembrane space into the cytoplasm via a permeability transition mechanisms [40]. The release mechanisms is believed to be accompanied by mitochondrial depolarisation that follows the mitochondrial permeability transition. Hence, one would assume that melatonin, being an mtPTP blocker, may preserve $\Delta\Psi_m$ in ischemic conditions. To test this assumption, we used an OGD model of neuronal cultures in conjunction with live cell imaging of the fluorescent dye TMRM that is selectively taken up in energized mitochondria. As expected, we found that the TMRM uptake in OGD-subjected cultures was strongly compromised compared to control cultures indicating that the noxious OGD stimulus leads to a decrease in $\Delta\psi_m$ as previously reported [156]. The protection against the OGD-induced loss of TMRM-uptake by CsA in our OGD model indicates the involvement of the mtPTP in the mitochondrial depolarisation. Indeed, melatonin also prevented the loss in TMRM uptake, which in turn

reflects the preservation of $\Delta\psi_m$. The TMRM uptake was not altered by melatonin in control cultures that were not subjected to OGD, indicating that melatonin exerts its effect only when pathological conditions like mtPTP formation prevail. It has been shown that CsA in addition to its effect on the mtPTP has the potential to inhibit also the multi drug resistance pump (MDR). This may cause changes in attaining the mitochondrial TMRM fluorescence in the cells that is independent of mtPTP action (for review, see [60]). Previously it was shown that the MDR inhibition by verapamil, that is also an MDR inhibitor, did not cause any alteration in the CsA-induced mitochondrial hyperpolarization [157]. If the component of MDR inhibition plays a role in our experimental model, one would assume that a treatment with verapamil results in a higher mitochondrial TMRM-uptake. Our results show that MDR inhibition by verapamil did not produce any change in attaining the mitochondrial TMRM-uptake. Furthermore, using different concentrations (50-200 nM, concentrations that are below the self-quenching threshold) of TMRM, showed no changes in mitochondrial fluorescence (data not shown), indicating, that an increased intracellular availability of TMRM as it would result from a MDR blockade, does not alter the baseline fluorescence in our model. Thus, our results show that a possible MDR inhibition in our model does not affect the mitochondrial TMRM uptake using our loading protocol. A large body of evidence suggests that the mtPTP is causally involved in the pathological changes following ischemia/reperfusion [59, 158]. Hence, a blockade of the mtPTP by melatonin may comprise a pharmacological strategy for the treatment of such pathological conditions.

During ischemia, the ATP level drops and the concentration of ADP and AMP increase due to the cessation of the mitochondrial oxidative phosphorylation [159]. Furthermore, tissue acidosis occurs during ischemia due to lactate accumulation [160]**.** Adenine nucleotides and low pH are potent blockers of the mtPTP [109], therefore it is unlikely that mtPTP opening occurs during the occlusion phase of stroke. Also, the uptake of cytosolic Ca^{2+} into mitochondria, being a pre-requisite for mtPTP formation is prevented by the mitochondrial depolarization that is initiated soon after the onset of the occlusion. However, during reperfusion, mitochondria become re-energized, hence the sequestration of Ca^{2+} that gets accumulated in the cytosol during ischemia [161] is reinstated. In addition, a shift towards a higher pH and excessive free radical generation has to be expected under such conditions [61, 62]. All these factors that occur during reperfusion favour the mtPTP formation. Accordingly, mitochondrial swelling as a result of permeability transition is observed in neurons within the first hours of reperfusion [162].

Taking into consideration that the reperfusion phase after ischemia is essential for the mtPTP opening, we choose to examine the effect of melatonin on the pathological changes in an MCAO model with 2 h occlusion followed by reperfusion. mtPTP-mediated brain injury has already been characterized in this MCAO model [163] and it was shown before that CsA treatment is protective in similar models of brain ischemia [111, 113]. Since CsA also inhibits calcineurin, one could assume that CsA may act as a protectant at least in part by utilizing this pathway. In most of these studies the neuroprotective effect of CsA was observed to be much more efficacious than that of FK506, an immunosuppressant that has an ability to inhibit calcineurin like CsA but has no effect of mtPTP. Moreover, N-methyl-valine-4-cyclosporine A (MeValCsA), a CsA analogue that has no effect on calcineurin, but blocks the mtPTP opening, has been shown to decrease the infarct volume in the MCAO model to the same extent as seen with CsA [164].

We used cyt c immunoreactivity in the cytosol as a marker for mtPTP activation in our MCAO model. It was shown before that such ischemia-induced cyt c release is blocked by CsA [165] indicating a mtPTP-dependent mechanism. Consistently we also observed high levels of cyt c immunoreactivity in the brain cytosol of MCAO-subjected rats at 4 h as well as at 24 h after the onset of reperfusion. We then proved our hypothesis that melatonin treatment reduces this increase in cytosolic cyt c immunoreactivity too, suggesting a lower mtPTP activity in presence of the drug. Such mtPTP-mediated cyt c release appears to be a feature also of other neuropathologies: CsA reduced the cyt c release from mitochondria in kainate-induced excitotoxicity in organotypic hippocampal cultures [166] and in neurons exposed to transient hypoglycemia [167]. Isolated brain mitochondria were shown to release cyt c in a mtPTP dependent mechanism when subjected to high Zn^{2+} levels [168] or to the neurotoxin MPP^{+}, used in experimental Parkinson models [169].

Some contradicting studies on isolated mitochondria suggest that the release of cyt c might occur also independently of the mtPTP. For example, Andreyev and Fiskum [42] showed that mtPTP-mediated cyt c release was found in liver but not in brain mitochondria suspensions. The discrepancy between these studies is not fully understood. It was suggested that the induction of mtPTP opening and subsequent cyt c release from brain mitochondria might require the intact tissue [42].

We followed the cascade of events that extends downstream from the mtPTP-mediated cyt c release by examining how melatonin affects the caspase-3 activation [167] and the subsequent DNA fragmentation [170]. Our MCAO model displayed an activation of

caspase-3 that was inhibited by melatonin consequentially also prevented the DNA fragmentation.

The melatonin-induced anti-apoptotic effects presented here are in agreement with other studies showing that melatonin inhibits apoptosis in ischemic kidney [171], in amyloid beta-peptide injury in hippocampal neurons [172] and NO-induced cell death in PGT-beta immortalized pineal cells [173]. It is interesting to note that melatonin is not protective in all models of apoptotic cell death [174], which may find its explanation in the fact that all the investigated noxious stimuli do not trigger mtPTP mediated apoptotic pathways. For example, melatonin does not protect against staurosporine-induced apoptosis, which is known to follow pathways that do not involve mitochondrial depolarization, hence the mtPTP is unlikely to be involved [175, 176].

Our *in-vivo* data do not rule out additionally to the direct mtPTP inhibition, an indirect effect of melatonin on the mtPTP activation by removing reactive nitrogen or oxygen species from the tissue. The clearly observed *in-vitro* actions of melatonin directly on the mtPTP may rather contribute to the overall outcome of its protective effect in *in-vivo* stroke models. The finding of a reduction in the infarct volume in our studies, is in agreement with previous results obtained by different authors that melatonin reduces the infarct size after cerebral ischemia [117-120] and serves here as a control for effectiveness of the MCAO insult.

The dose used in the present study is a pharmacological dose that has already been shown to cause neuroprotection in different models of neuronal degeneration [119, 177, 178]. The relevance of physiological melatonin levels in inhibiting brain damage due to ischemia / reperfusion in rats was confirmed by Kilic et al [179]. They showed that physiological melatonin concentrations are neuroprotective and also the pharmacological application effectively reduces the brain damage and improves the neurological status of ischemic rats. The findings that physiological melatonin concentrations are neuroprotective is of particular interest since endogenous levels of melatonin are diminished in many aged individuals; [180]. Thus, elderly individuals may be increasingly vulnerable to the damaging effects of a stroke because they lack the endogenous protectant melatonin. Melatonin is well known to modulate the activities of hypothalamic centers that regulate the circadian rhythm. Diurnal modulations of Ca^{2+} currents in the suprachiasmatic nucleus of the hypothalamus is reported to transduce the intracellular cycling of molecular clocks and circadian rhythm [181]. Since the mtPTP at its low-conductance state plays a role in the regulation of cellular Ca^{2+} homeostasis [152] one may speculate in the context of our

findings that melatonin could modulate such pathways. The results of the present study therefore open a new field for investigating other regulatory principles in melatonin controlled mechanisms. Taken together, our results demonstrate for the first time that melatonin directly inhibits the mtPTP and that this effect may contribute to the anti-apoptotic properties of melatonin. The direct inhibition of mtPTP provides an evidence for an alternative mechanism that is utilized by melatonin to offer neuroprotection. Being an antioxidant and inhibitor of the mtPTP, therapeutic intervention by melatonin may provide a beneficial clinical applications for the treatment of stroke and neurodegenerative disorders.

Melatonin, being safe and non-toxic, more experimental studies should be conducted to explore the synergetic actions of melatonin with other drugs, presently applied clinically.

4.2 OXY protects the neurons and inhibits apoptotic cell death in transient brain ischemia

In this study we provide evidence that OXY is a potent neuroprotectant in transient brain ischemia. In many clinical cases of stroke, reperfusion occurs after the occlusion phase spontaneously or is induced by pharmacological thrombolysis. Hence our MCAO model with a defined ischemic period and subsequent reperfusion resembles many features of the clinical situation in stroke patients [142, 182]. Moreover, middle cerebral artery, the specific occlusion site in this model, is the most commonly affected vessel in both embolic or thrombotic strokes in humans [3].

Here we show that an intraperitoneal application of a dose of 10 mg / kg OXY is sufficient to provide significant neuroprotection against MCAO-induced neuronal injury. This finding was supported by both histological and neurological data: we observed a reduction in the brain infarct volume after the ischemic insult and an attenuation of the neurological deficits, which are clinical features that are related to the life quality after stroke. OXY treatment reached, in our hands, a maximal protective capacity at a dose of 20 mg / kg, since no further neuroprotection was seen by increasing the dose to 30 mg / kg. A low dose of 2 mg / kg was not protective. To exclude indirect protective effects of OXY, for instance via alteration of the general physiological homeostasis like changes in blood pressure, body temperature or blood gas levels, which are known to affect the outcome of an ischemic insult [183, 184], we took great care to maintain these parameters at a constant level. Hence, the observed neuroprotection by OXY is apparently not attributed to such side effects.

We showed earlier in *in-vitro* studies that OXY is a potent antioxidant and scavenges ROS / RNS [131]. These findings include detoxifying effects for NO, H_2O_2 and $O_2^{\cdot-}$ [131, 185], species that are known to display strongly increased levels in the ischemic and post-ischemic brain [54-56]. It is commonly accepted that thereby induced oxidative / nitrosative stress plays a crucial role in the brain injury after ischemia / reperfusion (for review, see [54-56]). For example, activated microglial cells are identified as a source of elevated NO levels and other potentially pro-apoptotic factors in neuronal degeneration [139, 186-188]. In this context it is interesting to note that OXY inhibits LPS- and interferon-γ-induced microglial / macrophage activation and NO-output [131, 189]. Moreover, OXY was shown to remove such highly activated microglial cells from LPS-

and interferon-γ-treated primary mixed neuronal-glial mouse cultures that in turn contributes also to lower ROS / RNS levels. The neuroprotective effects by OXY may be explained by a combined effect of both, its antioxidative / antinitrosative actions and the decrease in ROS / RNS-producing microglial cell numbers.

Mitochondria are the cellular site that are prone to potentially harmful oxidative damage [190]. Such mitochondrial injury is reported to cause cyt c release into the cytosol that initiates the apoptotic cell death cascade [191]. OXY being a potent antioxidant, should interrupt this chain of events upstream of the mitochondrial damage by diminishing ROS / RNS concentrations. Here we used the cytosolic cyt c level as a marker to assess the effectiveness of cytoprotective action of OXY. Our results demonstrate that cyt c is released from the mitochondria into the cytosol within 4 h after reperfusion, indicating that ischemia / reperfusion may trigger mitochondrially-induced apoptosis, possibly by increasing the permeability of the mitochondrial membranes. At 24 h of reperfusion, cyt c was also seen extracellularly, showing that the cells get disrupted, whereby the contents including cyt c are shed-off into the extracellular space. In sham-operated rats, a low intensity - punctate pattern of the cyt c immunoreactivity, taken as an indicator of intact mitochondria, was observed. However, once released from the mitochondria, the cyt c signal is readily detectable. The reason for the low cyt-c immunofluorescence signal in intact mitochondria is partly attributed to the fixation procedure (as in our case with 4 % PFA) that hinders the antibody to reach the intermembrane space of mitochondria [192]. Another possible explanations are, that cyt c is densely packed into the intermembrane space that results in the commonly known phenomenon of collissional quenching of the fluorescence because the dye molecules reach a very high local concentration after the immunoreaction or that steric hinderance prevents the antibody from reaching the antigen. Also, once released into the cytosol, conformational changes occur in the cyt c molecule that leads to increased antibody binding to the protein [193] and in turn to a higher fluorescence signal. In any case, the strong cytosolic cyt c immunofluorescence is a suitable measure for mitochondrially released cyt c. OXY treatment in MCAO rats not only reduced such cytosolic cyt c staining at 4 h, but also decreased the extracellular label at 24 h, indicating a reduction of damage to the mitochondria. Along the line that cyt c release from mitochondria after ischemia / reperfusion activates the pro-apoptotic caspase-3 [51-53] , we show that MCAO-induced apoptosis was decreased by OXY treatment. Accordingly, immunohistochemical staining for caspase-3 as well as labeling of apoptotic-DNA was also found to be reduced after OXY treatment. Prevention of apoptotic cell death

by antioxidant application is in agreement with other studies [171, 194]. An increase in the expression of the endogenous antioxidant enzyme Cu / Zn-superoxide dismutase in rats yielded similar results by limiting cyt c release and caspase-3 activation and, thus, preventing subsequent apoptotic cell death in models of cerebral ischemia [192].

Taken together, we expanded on our previous *in-vitro* data [131] by demonstrating that OXY is also a potent neuroprotectant in an *in-vivo* model of stroke. From the results of the present study, we suggest that OXY may prove an excellent drug for the treatment of neurodegenerative disorders that causally involve oxidative / nitrosative stress, especially in stroke.

5. SUMMARY AND CONCLUSION

Focal brain ischemia caused by reduced supply of blood to cerebral tissue, results in cellular damage within the first few hours up to weeks after the insult. Extensive loss of neurons as well as glia in such ischemic brain areas is the characteristic pathological feature of cerebral infarcts causing mild to severe neurological symptoms that may even lead to the death of the subject. The cascade of events in the pathogenesis of stroke involves oxidative and nitrosative stress, i.e., the deleterious effects of reactive oxygen and nitrogen species (ROS / RNS).

It is known that RNS / ROS cause mitochondrial damage and lead to an accumulation of pro-apoptotic high cytosolic Ca^{2+} ($[Ca^{2+}]_c$) in the cells. It is now realised that an activation of the mitochondrial permeability transition pore (mtPTP), a megachannel formed in the mitochondrial membranes contributes to such pro-apoptotic $[Ca^{2+}]_c$ rise. Also, the mtPTP opening leads to the release of pro-apoptotic proteins like cytochrome c (cyt c), apoptosis inducing factor (AIF), Smac / DiaBLO and procaspases from the mitochondrial intermembrane space into the cytoplasm. The release of cyt c into the cytosol initiates the cascade of mitochondrial apoptotic cell death by activating caspase-3.

Treatment with drugs that can either directly inhibit the mtPTP or can reduced the oxidative / nitrosative stress are therefore potential pharmacological interventions to reduce the ischemia- induced brain injury.

5.1 Melatonin, the secretory product of the pineal gland, is known to be neuroprotective in cerebral ischemia, which is so far mostly attributed to its antioxidant properties. Here we show that melatonin directly inhibits the mtPTP. Consistently, NMDA-induced $[Ca^{2+}]_c$ rises were diminished by melatonin in cultured mouse striatal neurons, similar to the pattern seen with cyclosporine A (CsA), an inhibitor of mtPTP. When the mouse striatal neurons were subjected to oxygen-glucose deprivation (OGD), melatonin strongly prevented the OGD-induced loss of mitochondrial membrane potential. To assess the direct effect of melatonin on the mtPTP activity at the single channel level, recordings from the inner mitochondrial membrane were obtained by a patch-clamp approach using rat liver mitoplasts. Melatonin strongly inhibited mtPTP currents in a dose-dependent manner with an IC_{50} of 0.8 μM. If melatonin is an inhibitor of the mtPTP, it should prevent mitochondrial cyt c release as seen in stroke models. Rats underwent middle cerebral artery

occlusion (MCAO) for 2 h followed by reperfusion. Melatonin (10 mg/kg intrapertoneal, i.p.) or vehicle was given at the time of occlusion and at the time of reperfusion. Indeed, infarct area in the brain sections of melatonin-treated animals displayed a considerably decreased cyt c release along with less activation of caspase-3 and apoptotic DNA fragmentation. Melatonin treatment diminished the loss of neurons and decreased the infarct volume as compared to vehicle-treated MCAO rats. Our findings suggest that the direct inhibition of the mtPTP by melatonin may essentially contribute to its anti-apoptotic effects in transient brain ischemia.

5.2 Since oxidative / nitrosative stress is one of the major pathological factors in the cascade of cell death in cerebral ischemia, we investigated the neuroprotective effect of a naturally occurring antioxidant, oxyresveratrol (OXY) to reduce brain injury after cerebral stroke. We used the MCAO model of transient brain ischemia to induce a defined brain infarction. OXY was given twice i.p.: immediately after occlusion and at the time of reperfusion. OXY (10 or 20 mg / kg) significantly reduced the brain infarct volume by approximately 54 ± 4 % and 63 ± 5 %, respectively, when compared to vehicle-treated MCAO rats. Also, the neurological deficits as assessed by different scoring methods reduced in OXY-treated MCAO rats. Histological analysis of apoptotic markers in the ischemic brain area revealed that OXY treatment diminished cyt c release from the mitochondria and decreased caspase-3 activation in MCAO rats. Also, staining for apoptotic DNA showed that the number of apoptotic nuclei in ischemic brain were reduced after OXY treatment as compared to the vehicle-treated MCAO rats. These findings demonstrate that OXY is neuroprotective in an *in-vivo* stroke model by limiting ischemia-induced brain injury.

Taken together, we show here for the first time that the endogenous pineal hormone melatonin is a blocker of the mtPTP. Our data indicate that this property of melatonin contributes to its neuroprotective effects both, *in-vitro* and *in-vivo.*

Furthermore, we established the naturally occurring hydroxystilbene, OXY as a potent neuroprotectant in a transient brain ischemia model, by demonstrating strongly reduced infarct volumes and neurological deficits upon its treatment after stroke insults.

Our data show that both melatonin and OXY are potential drugs for the development of pharmacological intervention in stroke therapy.

6. ZUSAMMENFASSUNG

Eine fokale Ischämie des Zentralnervensystems wird durch die reduzierte Blutversorgung eines distinkten cerebralen Hirnareals verursacht. Das führt zu massiven Zellschädigungen innerhalb der ersten Stunden bis zu Wochen nach dem Insult. Der extensive Verlust von Neuronen und Gliazellen in einem von Ischämie betroffenen Areal ist das pathologische Hauptcharakteristikum eines Schlaganfalls und führt - je nach Ausmaß und Lokalisation - zu neurologischen Symptomen verschiedener Schweregrade bis hin zum Tode des Patienten. In der Ereigniskaskade der Pathogenese des Schlaganfalls spielt oxidativer und nitrosativer Stress eine wichtige Rolle, hervorgerufen durch die schädigenden Effekte von reaktiven Stickstoff- und Sauerstoffspezies (ROS/RNS). Es ist bekannt, dass RNS/ROS einen direkt schädigenden Einfluß auf Mitochondrien ausüben und zu einer potentiell proapoptotischen Akkumulation von Ca^{2+} im Zytosol ($[Ca^{2+}]_c$) führen können. Zu diesem proapoptotische Anstieg des $[Ca^{2+}]_c$ trägt wahrscheinlich die Aktivierung der mitochondrialen *permeability transition pore* (mtPTP) bei, einem Megakanal, der sich durch die innere und äußere Membran der Mitochondrien spannt. Durch die mtPTP können auch proapoptotische Proteine, wie Cytochrom C (cyt c), *apoptosis inducing factor* (AIF), Smac/DiaBLO und Procaspasen, aus dem Intermembranraum in das Zytosol gelangen. Die Freisetzung von cyt c in das Zytosol initiiert die mitochondriale apoptotische Zelltodkaskade über eine Aktivierung von Caspase-3. Die Behandlung cerebraler Ischämie mit Substanzen, die entweder die mtPTP direkt inhibieren oder die den oxidativen/nitrosativen Stress reduzieren, erscheint von besonderem Interesse, weil von einer solchen pharmakologischen Intervention zur Reduzierung der durch Ischämie-verursachten Hirnschädigung eine entsprechende Wirksamkeit erwartet werden kann.

Die der Dissertation zugrunde liegenden Untersuchungen konzentrieren sich zunächst auf Melatonin. Melatonin ist ein Amin, das von Zellen des Pinealorgans synthetisiert und sezerniert wird. Es wird als Neuroprotektivum im Zusammenhang mit cerebraler Ischämie diskutiert, wobei die Wirkung hauptsächlich seinen antioxidativen Eigenschaften zugeschrieben wird. Hier wird erstmalig gezeigt, dass Melatonin die mtPTP direkt inhibieren kann. Übereinstimmend damit belegen die weiteren Ergebnisse, dass der NMDA-induzierte $[Ca^{2+}]_c$-Anstieg in striatalen Maus-Neuronenkulturen durch Melatonin reduziert wird, ähnlich der Wirkung, die man bei Behandlung mit Cyclosporin A (CsA), einem Blocker der mtPTP, beobachtet. Wenn solche Neuronenkulturen einem Sauerstoff-

Glukose-Entzug (OGD) ausgesetzt wurden, dann war Melatonin in der Lage, den durch OGD verursachten Verlust des mitochondrialen Membranpotentials zu verhindern. Um den direkten Effekt von Melatonin auf die mtPTP-Aktivität auf Einzelkanalebene zu ermitteln, wurde in elektrophysiologischen *patch-clamp* Studien die mtPTP-Aktivität an der inneren mitochondrialen Membran von Lebermitoplasten aufgezeichnet. Dabei zeigte sich, dass Melatonin dosisabhängig die mtPTP-Ströme mit einem IC_{50} von 0,8 µM inhibiert.

Auf der Basis dieser Ergebnisse kann vermutet werden, dass Melatonin als wirksamer mtPTP-Blocker die Freisetzung von cyt c aus Mitochondrien in das Zytosol, analog zu der des Ca^{2+}, verhindert. Für eine entsprechende Untersuchung am Ganztier benutzten wir das *middle cerebral artery occlusion (MCAO)*-Modell, bei dem in Ratten die A*rteria media cerebri* für zwei Stunden mit nachfolgender Reperfusion okkludiert wird. Melatonin (10 mg/kg, i. p.) oder die entsprechende Vehikel-Lösung wurden wiederholt appliziert: einmal nach der Okklusion und einmal zum Zeitpunkt der Reperfusion. Tatsächlich zeigte das Infarktareal in Hirnschnitten von Melatonin-behandelten Tieren eine stark verringerte cyt c- Immunoreaktivität im Zytosol, begleitet von einer reduzierten Aktivierung von Caspase 3 und apoptotischer DNA-Fragmentierung. Melatonin verringerte auch den Verlust von Neuronen und reduzierte das Infarktvolumen im Vergleich zu Vehikel-behandelten MCAO-Ratten ganz beträchtlich. Unsere Befunde implizieren, dass die direkte Inhibierung der mtPTP durch Melatonin essentiell zum antiapoptotischen Effekt dieser Substanz bei transienter Hirnischämie beiträgt.

Da oxidativer/nitrosativer Stress ein pathologischer Hauptfaktor in der apoptotischen Kaskade der cerebralen Ischämie ist, wurde weiteres natürlich vorkommendes Antioxidants, das Oxyresveratrol (OXY), untersucht in Bezug auf seinen potentiellen neuroprotektiven Effekt. Erneut kam dazu das MCAO-Modell transienter Hirnischämie zum Einsatz. OXY wurde wiederholt i. p. appliziert: einmal sofort nach Okklusion und einmal zum Zeitpunkt der Reperfusion. 10 bzw. 20 mg/kg OXY reduzierten das Hirninfarktvolumen im Vergleich zu Vehikel-behandelten MCAO-Ratten um mehr als die Hälfte (um 54 ± 4% bzw. 63 ± 5 %). Auch die neurologischen Defizite, die anhand verschiedener Verhaltensparameter erfasst wurden, waren in OXY-behandelten MCAO-Ratten geringer ausgeprägt. Die histologische Analyse von Apoptose-Markern im ischämischen Hirnareal zeigte, dass OXY die cyt c-Freisetzung aus Mitochondrien und die nachfolgende Caspase-3-Aktivierung in MCAO-Ratten verringerte. Zudem reduzierte OXY die Anzahl der sich in Apoptose befindenden Zellen im ischämischen Hirnareal im Vergleich zu Vehikel-behandelten MCAO-Ratten, wie unter Verwendung von Antikörpern

gegen apoptotische Einzelstrang-DNA nachgewiesen werden konnte. Diese Befunde belegen in dem von uns verwendeten *in-vivo*-Schlaganfall-Modell, dass OXY nach akuter Hirnischämie zur Verringerung der Schädigung des Hirngewebes führt.

Befunde, die in der Dissertation, wie auch in den daraus resultierenden Publikationen vorgestellt wurden, belegen, dass sowohl Melatonin als auch OXY, interessante Kandidaten für eine erfolgreiche Intervention in der Schlaganfall-Therapie sind.

7. REFERENCES

1. Bhardwaj, A., et al., *Mechanisms of ischemic brain damage.* Curr Cardiol Rep, 2003. **5**(2): p. 160-7.
2. Iadecola, C., *Neurogenic control of the cerebral microcirculation: is dopamine minding the store?* Nat Neurosci, 1998. **1**(4): p. 263-5.
3. Scatton, B., *Excitatory amino acid receptor antagonists: a novel treatment for ischemic cerebrovascular diseases.* Life Sci, 1994. **55**(25-26): p. 2115-24.
4. Wallimann, T., et al., *Intracellular compartmentation, structure and function of creatine kinase isoenzymes in tissues with high and fluctuating energy demands: the 'phosphocreatine circuit' for cellular energy homeostasis.* Biochem J, 1992. **281 (Pt 1)**: p. 21-40.
5. Martin, R.L., H.G. Lloyd, and A.I. Cowan, *The early events of oxygen and glucose deprivation: setting the scene for neuronal death?* Trends Neurosci, 1994. **17**(6): p. 251-7.
6. Hossmann, K.A., *Viability thresholds and the penumbra of focal ischemia.* Ann Neurol, 1994. **36**(4): p. 557-65.
7. Linnik, M.D., R.H. Zobrist, and M.D. Hatfield, *Evidence supporting a role for programmed cell death in focal cerebral ischemia in rats.* Stroke, 1993. **24**(12): p. 2002-8; discussion 2008-9.
8. Guegan, C., et al., *Recruitment of several neuroprotective pathways after permanent focal ischemia in mice.* Exp Neurol, 1998. **154**(2): p. 371-80.
9. Charriaut-Marlangue, C., et al., *Apoptosis and necrosis after reversible focal ischemia: an in situ DNA fragmentation analysis.* J Cereb Blood Flow Metab, 1996. **16**(2): p. 186-94.
10. Wyllie, A.H., J.F. Kerr, and A.R. Currie, *Cell death: the significance of apoptosis.* Int Rev Cytol, 1980. **68**: p. 251-306.
11. Wyllie, A.H., G.J. Beattie, and A.D. Hargreaves, *Chromatin changes in apoptosis.* Histochem J, 1981. **13**(4): p. 681-92.

12. Lipton, P., *Ischemic cell death in brain neurons.* Physiol Rev, 1999. **79**(4): p. 1431-568.
13. Martin, L.J., et al., *Neurodegeneration in excitotoxicity, global cerebral ischemia, and target deprivation: A perspective on the contributions of apoptosis and necrosis.* Brain Res Bull, 1998. **46**(4): p. 281-309.
14. Portera-Cailliau, C., D.L. Price, and L.J. Martin, *Non-NMDA and NMDA receptor-mediated excitotoxic neuronal deaths in adult brain are morphologically distinct: further evidence for an apoptosis-necrosis continuum.* J Comp Neurol, 1997. **378**(1): p. 88-104.
15. Choi, D.W. and F.H. Gage, *Disease, transplantation and regeneration.* Curr Opin Neurobiol, 1996. **6**(5): p. 635-7.
16. Choi, D.W., *Ischemia-induced neuronal apoptosis.* Curr Opin Neurobiol, 1996. **6**(5): p. 667-72.
17. Gwag, B.J., et al., *Blockade of glutamate receptors unmasks neuronal apoptosis after oxygen-glucose deprivation in vitro.* Neuroscience, 1995. **68**(3): p. 615-9.
18. Leist, M., et al., *Intracellular adenosine triphosphate (ATP) concentration: a switch in the decision between apoptosis and necrosis.* J Exp Med, 1997. **185**(8): p. 1481-6.
19. Melino, G., et al., *Nitric oxide can inhibit apoptosis or switch it into necrosis.* Cell Mol Life Sci, 2000. **57**(4): p. 612-22.
20. Hata, R., et al., *A reproducible model of middle cerebral artery occlusion in mice: hemodynamic, biochemical, and magnetic resonance imaging.* J Cereb Blood Flow Metab, 1998. **18**(4): p. 367-75.
21. Yao, H., et al., *DNA fragmentation in ischemic core and penumbra in focal cerebral ischemia in rats.* Brain Res Mol Brain Res, 2001. **91**(1-2): p. 112-8.
22. Manabat, C., et al., *Reperfusion differentially induces caspase-3 activation in ischemic core and penumbra after stroke in immature brain.* Stroke, 2003. **34**(1): p. 207-13.
23. Zeng, Y.S. and Z.C. Xu, *Co-existence of necrosis and apoptosis in rat hippocampus following transient forebrain ischemia.* Neurosci Res, 2000. **37**(2): p. 113-25.
24. Earnshaw, W.C., *Apoptosis. A cellular poison cupboard.* Nature, 1999. **397**(6718): p. 387, 389.

25. Strasser, A., L. O'Connor, and V.M. Dixit, *Apoptosis signaling.* Annu Rev Biochem, 2000. **69**: p. 217-45.

26. Kaufmann, S.H. and M.O. Hengartner, *Programmed cell death: alive and well in the new millennium.* Trends Cell Biol, 2001. **11**(12): p. 526-34.

27. Soldani, C. and A.I. Scovassi, *Poly(ADP-ribose) polymerase-1 cleavage during apoptosis: an update.* Apoptosis, 2002. **7**(4): p. 321-8.

28. Sakahira, H., M. Enari, and S. Nagata, *Cleavage of CAD inhibitor in CAD activation and DNA degradation during apoptosis.* Nature, 1998. **391**(6662): p. 96-9.

29. Enari, M., et al., *A caspase-activated DNase that degrades DNA during apoptosis, and its inhibitor ICAD.* Nature, 1998. **391**(6662): p. 43-50.

30. Hermann, D.M., et al., *Adenovirus-mediated glial cell line-derived neurotrophic factor (GDNF) expression protects against subsequent cortical cold injury in rats.* Neurobiol Dis, 2001. **8**(6): p. 964-73.

31. Namura, S., et al., *Activation and cleavage of caspase-3 in apoptosis induced by experimental cerebral ischemia.* J Neurosci, 1998. **18**(10): p. 3659-68.

32. Gillardon, F., et al., *Inhibition of caspases prevents cell death of hippocampal CA1 neurons, but not impairment of hippocampal long-term potentiation following global ischemia.* Neuroscience, 1999. **93**(4): p. 1219-22.

33. Cao, G., et al., *Caspase-activated DNase/DNA fragmentation factor 40 mediates apoptotic DNA fragmentation in transient cerebral ischemia and in neuronal cultures.* J Neurosci, 2001. **21**(13): p. 4678-90.

34. Luo, Y., et al., *Induction of caspase-activated deoxyribonuclease activity after focal cerebral ischemia and reperfusion.* J Cereb Blood Flow Metab, 2002. **22**(1): p. 15-20.

35. Krupinski, J., et al., *Expression of caspases and their substrates in the rat model of focal cerebral ischemia.* Neurobiol Dis, 2000. **7**(4): p. 332-42.

36. Chen, J., et al., *Induction of caspase-3-like protease may mediate delayed neuronal death in the hippocampus after transient cerebral ischemia.* J Neurosci, 1998. **18**(13): p. 4914-28.

37. Endres, M., et al., *Attenuation of delayed neuronal death after mild focal ischemia in mice by inhibition of the caspase family.* J Cereb Blood Flow Metab, 1998. **18**(3): p. 238-47.

38. Fink, K., et al., *Prolonged therapeutic window for ischemic brain damage caused by delayed caspase activation.* J Cereb Blood Flow Metab, 1998. **18**(10): p. 1071-6.

39. Love, S., *Apoptosis and brain ischaemia.* Prog Neuropsychopharmacol Biol Psychiatry, 2003. **27**(2): p. 267-82.

40. Wang, X., *The expanding role of mitochondria in apoptosis.* Genes Dev, 2001. **15**(22): p. 2922-33.

41. Qian, T., B. Herman, and J.J. Lemasters, *The mitochondrial permeability transition mediates both necrotic and apoptotic death of hepatocytes exposed to Br-A23187.* Toxicol Appl Pharmacol, 1999. **154**(2): p. 117-25.

42. Andreyev, A. and G. Fiskum, *Calcium induced release of mitochondrial cytochrome c by different mechanisms selective for brain versus liver.* Cell Death Differ, 1999. **6**(9): p. 825-32.

43. Scorrano, L. and S.J. Korsmeyer, *Mechanisms of cytochrome c release by proapoptotic BCL-2 family members.* Biochem Biophys Res Commun, 2003. **304**(3): p. 437-44.

44. Cao, G., et al., *Intracellular Bax translocation after transient cerebral ischemia: implications for a role of the mitochondrial apoptotic signaling pathway in ischemic neuronal death.* J Cereb Blood Flow Metab, 2001. **21**(4): p. 321-33.

45. Fujimura, M., et al., *Cytosolic redistribution of cytochrome c after transient focal cerebral ischemia in rats.* J Cereb Blood Flow Metab, 1998. **18**(11): p. 1239-47.

46. Krajewski, S., et al., *Release of caspase-9 from mitochondria during neuronal apoptosis and cerebral ischemia.* Proc Natl Acad Sci U S A, 1999. **96**(10): p. 5752-7.

47. Fujimura, M., et al., *Manganese superoxide dismutase mediates the early release of mitochondrial cytochrome C and subsequent DNA fragmentation after permanent focal cerebral ischemia in mice.* J Neurosci, 1999. **19**(9): p. 3414-22.

48. Guegan, C. and B. Sola, *Early and sequential recruitment of apoptotic effectors after focal permanent ischemia in mice.* Brain Res, 2000. **856**(1-2): p. 93-100.

49. Gonzales, D.H. and W. Neupert, *Biogenesis of mitochondrial c-type cytochromes.* J Bioenerg Biomembr, 1990. **22**(6): p. 753-68.

50. Yang, J., et al., *Prevention of apoptosis by Bcl-2: release of cytochrome c from mitochondria blocked.* Science, 1997. **275**(5303): p. 1129-32.

51. Green, D.R. and J.C. Reed, *Mitochondria and apoptosis.* Science, 1998. **281**(5381): p. 1309-12.

52. Liu, X., et al., *Induction of apoptotic program in cell-free extracts: requirement for dATP and cytochrome c.* Cell, 1996. **86**(1): p. 147-57.

53. Martinou, J.C. and D.R. Green, *Breaking the mitochondrial barrier.* Nat Rev Mol Cell Biol, 2001. **2**(1): p. 63-7.

54. McCord, J.M., *Oxygen-derived free radicals in postischemic tissue injury.* N Engl J Med, 1985. **312**(3): p. 159-63.

55. Chan, P.H., *Reactive oxygen radicals in signaling and damage in the ischemic brain.* J Cereb Blood Flow Metab, 2001. **21**(1): p. 2-14.

56. Lewen, A., P. Matz, and P.H. Chan, *Free radical pathways in CNS injury.* J Neurotrauma, 2000. **17**(10): p. 871-90.

57. Ikeda, Y. and D.M. Long, *The molecular basis of brain injury and brain edema: the role of oxygen free radicals.* Neurosurgery, 1990. **27**(1): p. 1-11.

58. Kroemer, G. and J.C. Reed, *Mitochondrial control of cell death.* Nat Med, 2000. **6**(5): p. 513-9.

59. Crompton, M., *The mitochondrial permeability transition pore and its role in cell death.* Biochem J, 1999. **341**(Pt 2): p. 233-49.

60. Bernardi, P., et al., *A mitochondrial perspective on cell death.* Trends Biochem Sci, 2001. **26**(2): p. 112-7.

61. Back, T., et al., *Penumbral tissue alkalosis in focal cerebral ischemia: relationship to energy metabolism, blood flow, and steady potential.* Ann Neurol, 2000. **47**(4): p. 485-92.

62. Piantadosi, C.A. and J. Zhang, *Mitochondrial generation of reactive oxygen species after brain ischemia in the rat.* Stroke, 1996. **27**(2): p. 327-31; discussion 332.

63. Palmer, C., *Hypoxic-ischemic encephalopathy. Therapeutic approaches against microvascular injury, and role of neutrophils, PAF, and free radicals.* Clinics In Perinatology, 1995. **22**(2): p. 481-517.

64. Contestabile, A., B. Monti, and E. Ciani, *Brain nitric oxide and its dual role in neurodegeneration/neuroprotection: understanding molecular mechanisms to devise drug approaches.* Curr Med Chem, 2003. **10**(20): p. 2147-74.

65. Crow, J.P. and J.S. Beckman, *The role of peroxynitrite in nitric oxide-mediated toxicity.* Current Topics In Microbiology And Immunology, 1995. **196**: p. 57-73.

66. Murphy, A.N., G. Fiskum, and M.F. Beal, *Mitochondria in neurodegeneration: bioenergetic function in cell life and death.* J Cereb Blood Flow Metab, 1999. **19**(3): p. 231-45.

67. Chan, P.H., *Oxygen radicals in focal cerebral ischemia.* Brain Pathol, 1994. **4**(1): p. 59-65.

68. Levine, W.G., *Glutathione, lipid peroxidation and regulation of cytochrome P-450 activity.* Life Sci, 1982. **31**(8): p. 779-84.

69. Hattori, I., et al., *Intravenous administration of thioredoxin decreases brain damage following transient focal cerebral ischemia in mice.* Antioxid Redox Signal, 2004. **6**(1): p. 81-7.

70. Dawson, T.M. and V.L. Dawson, *Molecular pathways of neurodegeneration in Parkinson's disease.* Science, 2003. **302**(5646): p. 819-22.

71. Simonian, N.A. and J.T. Coyle, *Oxidative stress in neurodegenerative diseases.* Annu Rev Pharmacol Toxicol, 1996. **36**: p. 83-106.

72. Keller, J.N., et al., *Mitochondrial manganese superoxide dismutase prevents neural apoptosis and reduces ischemic brain injury: suppression of peroxynitrite production, lipid peroxidation, and mitochondrial dysfunction.* J Neurosci, 1998. **18**(2): p. 687-97.

73. Murakami, K., et al., *Mitochondrial susceptibility to oxidative stress exacerbates cerebral infarction that follows permanent focal cerebral ischemia in mutant mice with manganese superoxide dismutase deficiency.* J Neurosci, 1998. **18**(1): p. 205-13.

74. Kim, G.W., et al., *Manganese superoxide dismutase deficiency exacerbates cerebral infarction after focal cerebral ischemia/reperfusion in mice: implications for the production and role of superoxide radicals.* Stroke, 2002. **33**(3): p. 809-15.

75. Hasegawa, K., et al., *Direct measurement of free radicals in the neonatal mouse brain subjected to hypoxia: an electron spin resonance spectroscopic study.* Brain Research, 1993. **607**(1-2): p. 161-166.

76. Armstead, W.M., et al., *Postischemic generation of superoxide anion by newborn pig brain.* The American Journal Of Physiology, 1988. **255**(2): p. H401-H403.

77. Bagenholm, R., P. Andine, and H. Hagberg, *Effects of the 21-amino steroid tirilazad mesylate (U-74006F) on brain damage and edema after perinatal hypoxia-ischemia in the rat.* Pediatric Research, 1996. **40**(3): p. 399-403.

78. Palmer, C., et al., *Allopurinol administered after inducing hypoxia-ischemia reduces brain injury in 7-day-old rats.* Pediatric Research, 1993. **33**(1): p. 405-411.

79. Palmer, C., R.L. Roberts, and C. Bero, *Deferoxamine posttreatment reduces ischemic brain injury in neonatal rats.* Stroke; a Journal Of Cerebral Circulation, 1994. **25**(5): p. 1039-1045.

80. Huang, Z., et al., *Effects of cerebral ischemia in mice deficient in neuronal nitric oxide synthase.* Science, 1994. **265**(5180): p. 1883-1885.

81. Iadecola, C., F. Zhang, and X. Xu, *Inhibition of inducible nitric oxide synthase ameliorates cerebral ischemic damage.* The American Journal Of Physiology, 1995. **268**(2): p. R286-R292.

82. Ikeda, K., H. Negishi, and Y. Yamori, *Antioxidant nutrients and hypoxia/ischemia brain injury in rodents.* Toxicology, 2003. **189**(1-2): p. 55-61.

83. Skaper, S.D., et al., *Excitotoxicity, oxidative stress, and the neuroprotective potential of melatonin.* Ann N Y Acad Sci, 1999. **890**: p. 107-18.

84. Shimizu-Sasamata, M., et al., *Attenuated neurotransmitter release and spreading depression-like depolarizations after focal ischemia in mutant mice with disrupted type I nitric oxide synthase gene.* J Neurosci, 1998. **18**(22): p. 9564-71.

85. Cao, G., et al., *In Vivo Delivery of a Bcl-xL Fusion Protein Containing the TAT Protein Transduction Domain Protects against Ischemic Brain Injury and Neuronal Apoptosis.* J Neurosci, 2002. **22**(13): p. 5423-31.

86. Danbolt, N.C., *Glutamate uptake.* Prog Neurobiol, 2001. **65**(1): p. 1-105.

87. Hollmann, M. and S. Heinemann, *Cloned glutamate receptors.* Annu Rev Neurosci, 1994. **17**: p. 31-108.

88. Berridge, M.J., P. Lipp, and M.D. Bootman, *The versatility and universality of calcium signalling.* Nat Rev Mol Cell Biol, 2000. **1**(1): p. 11-21.

89. Hajnoczky, G., et al., *Control of apoptosis by IP3and ryanodine receptor driven calcium signals.* Cell Calcium, 2000. **28**(5-6): p. 349-363.

90. Szalai, G., R. Krishnamurthy, and G. Hajnoczky, *Apoptosis driven by IP3-linked mitochondrial calcium signals.* EMBO J., 1999. **18**(22): p. 6349-6361.

91. Scorrano, L., et al., *BAX and BAK Regulation of Endoplasmic Reticulum Ca2+: A Control Point for Apoptosis.* Science, 2003. **300**(5616): p. 135-139.

92. Fleckenstein, A., et al., *Myocardial fiber necrosis due to intracellular Ca overload-a new principle in cardiac pathophysiology.* Recent Adv Stud Cardiac Struct Metab, 1974. **4**: p. 563-80.

93. Wrogemann, K. and S.D. Pena, *Mitochondrial calcium overload: A general mechanism for cell-necrosis in muscle diseases.* Lancet, 1976. **1**(7961): p. 672-4.

94. Leonard, J.P. and M.M. Salpeter, *Agonist-induced myopathy at the neuromuscular junction is mediated by calcium.* J Cell Biol, 1979. **82**(3): p. 811-9.

95. Hajnoczky, G., E. Davies, and M. Madesh, *Calcium signaling and apoptosis.* Biochem Biophys Res Commun, 2003. **304**(3): p. 445-54.

96. Kristian, T. and B.K. Siesjo, *Calcium in ischemic cell death.* Stroke, 1998. **29**(3): p. 705-18.

97. Carafoli, E., *Calcium signaling: a tale for all seasons.* Proc Natl Acad Sci U S A, 2002. **99**(3): p. 1115-22.

98. Gunter, T.E. and D.R. Pfeiffer, *Mechanisms by which mitochondria transport calcium.* Am J Physiol, 1990. **258**(5 Pt 1): p. C755-86.

99. Gunter, T.E., et al., *Mitochondrial calcium transport: physiological and pathological relevance.* Am J Physiol, 1994. **267**(2 Pt 1): p. C313-39.

100. Mitchell, P., *Chemiosmotic coupling in oxidative and photosynthetic phosphorylation.* Biol Rev Camb Philos Soc, 1966. **41**(3): p. 445-502.

101. Crompton, M. and I. Heid, *The cycling of calcium, sodium, and protons across the inner membrane of cardiac mitochondria.* Eur J Biochem, 1978. **91**(2): p. 599-608.

102. Crompton, M., M. Kunzi, and E. Carafoli, *The calcium-induced and sodium-induced effluxes of calcium from heart mitochondria. Evidence for a sodium-calcium carrier.* Eur J Biochem, 1977. **79**(2): p. 549-58.

103. Bernardi, P., et al., *Mitochondria and cell death. Mechanistic aspects and methodological issues.* Eur J Biochem, 1999. **264**(3): p. 687-701.

104. Kroemer, G., *Mitochondrial control of apoptosis: an overview.* Biochem Soc Symp, 1999. **66**: p. 1-15.

105. Crompton, M., H. Ellinger, and A. Costi, *Inhibition by cyclosporin A of a Ca2+-dependent pore in heart mitochondria activated by inorganic phosphate and oxidative stress.* Biochem J, 1988. **255**(1): p. 357-60.

106. Duchen, M.R., et al., *On the involvement of a cyclosporin A sensitive mitochondrial pore in myocardial reperfusion injury.* Cardiovasc Res, 1993. **27**(10): p. 1790-4.

107. Richter, C., *Pro-oxidants and mitochondrial Ca2+: their relationship to apoptosis and oncogenesis.* FEBS Lett, 1993. **325**(1-2): p. 104-7.

108. Richter, C., et al., *Oxidants in mitochondria: from physiology to diseases.* Biochim Biophys Acta, 1995. **1271**(1): p. 67-74.

109. Halestrap, A.P., *The mitochondrial permeability transition: its molecular mechanism and role in reperfusion injury.* Biochem Soc Symp, 1999. **66**: p. 181-203.

110. Halestrap, A.P., et al., *Elucidating the molecular mechanism of the permeability transition pore and its role in reperfusion injury of the heart.* Biochim Biophys Acta, 1998. **1366**(1-2): p. 79-94.

111. Uchino, H., et al., *Differential neuroprotection by cyclosporin A and FK506 following ischemia corresponds with differing abilities to inhibit calcineurin and the mitochondrial permeability transition.* Neurobiol Dis, 2002. **10**(3): p. 219-33.

112. Uchino, H., et al., *Amelioration by cyclosporin A of brain damage in transient forebrain ischemia in the rat.* Brain Res, 1998. **812**(1-2): p. 216-26.

113. Yoshimoto, T. and B.K. Siesjo, *Posttreatment with the immunosuppressant cyclosporin A in transient focal ischemia.* Brain Res, 1999. **839**(2): p. 283-91.

114. Davenport, R. and M. Dennis, *Neurological emergencies: acute stroke.* J Neurol Neurosurg Psychiatry, 2000. **68**(3): p. 277-88.

115. Furlan, A., et al., *Intra-arterial prourokinase for acute ischemic stroke. The PROACT II study: a randomized controlled trial. Prolyse in Acute Cerebral Thromboembolism.* Jama, 1999. **282**(21): p. 2003-11.

116. Tan, D.X., et al., *Significance of melatonin in antioxidative defense system: reactions and products.* Biol Signals Recept, 2000. **9**(3-4): p. 137-59.

117. Pei, Z., S.F. Pang, and R.T. Cheung, *Pretreatment with melatonin reduces volume of cerebral infarction in a rat middle cerebral artery occlusion stroke model.* J Pineal Res, 2002. **32**(3): p. 168-72.

118. Pei, Z., S.F. Pang, and R.T. Cheung, *Administration of melatonin after onset of ischemia reduces the volume of cerebral infarction in a rat middle cerebral artery occlusion stroke model.* Stroke, 2003. **34**(3): p. 770-5.

119. Cho, S., et al., *Melatonin administration protects CA1 hippocampal neurons after transient forebrain ischemia in rats.* Brain Res, 1997. **755**(2): p. 335-8.

120. Manev, H., et al., *Increased brain damage after stroke or excitotoxic seizures in melatonin-deficient rats.* Faseb J, 1996. **10**(13): p. 1546-51.

121. Joo, W.S., et al., *Melatonin increases striatal dopaminergic function in 6-OHDA-lesioned rats.* Neuroreport, 1998. **9**(18): p. 4123-6.

122. Acuna-Castroviejo, D., et al., *Melatonin is protective against MPTP-induced striatal and hippocampal lesions.* Life Sci, 1997. **60**(2): p. PL23-9.

123. Lapin, I.P., et al., *Anticonvulsant activity of melatonin against seizures induced by quinolinate, kainate, glutamate, NMDA, and pentylenetetrazole in mice.* J Pineal Res, 1998. **24**(4): p. 215-8.

124. Huerto-Delgadillo, L., F. Anton-Tay, and G. Benitez-King, *Effects of melatonin on microtubule assembly depend on hormone concentration: role of melatonin as a calmodulin antagonist.* J Pineal Res, 1994. **17**(2): p. 55-62.

125. Barlow-Walden, L.R., et al., *Melatonin stimulates brain glutathione peroxidase activity.* Neurochem Int, 1995. **26**(5): p. 497-502.

126. Antolin, I., et al., *Neurohormone melatonin prevents cell damage: effect on gene expression for antioxidant enzymes.* Faseb J, 1996. **10**(8): p. 882-90.

127. Mohan, N., et al., *The neurohormone melatonin inhibits cytokine, mitogen and ionizing radiation induced NF-kappa B.* Biochem Mol Biol Int, 1995. **37**(6): p. 1063-70.

128. Gilad, E., et al., *Melatonin inhibits expression of the inducible isoform of nitric oxide synthase in murine macrophages: role of inhibition of NFkappaB activation.* Faseb J, 1998. **12**(9): p. 685-93.

129. Fremont, L., *Biological effects of resveratrol.* Life Sci, 2000. **66**(8): p. 663-73.

130. Hung, L.M., et al., *Beneficial effects of astringinin, a resveratrol analogue, on the ischemia and reperfusion damage in rat heart.* Free Radic Biol Med, 2001. **30**(8): p. 877-83.

131. Lorenz, P., et al., *Oxyresveratrol and resveratrol are potent antioxidants and free radical scavengers: effect on nitrosative and oxidative stress derived from microglial cells.* Nitric Oxide, 2003. **9**(2): p. 64-76.

132. Wang, Q., et al., *Resveratrol protects against global cerebral ischemic injury in gerbils.* Brain Research, 2002. **958**(2): p. 439-447.

133. Huang, S.S., et al., *Resveratrol reduction of infarct size in Long-Evans rats subjected to focal cerebral ischemia.* Life Sci, 2001. **69**(9): p. 1057-65.

134. Qiu, F., et al., *Pharmacological properties of traditional medicines. XXII. Pharmacokinetic study of mulberroside A and its metabolites in rat.* Biol Pharm Bull, 1996. **19**(11): p. 1463-7.

135. Kim, Y.M., et al., *Oxyresveratrol and hydroxystilbene compounds : Inhibitory effect on tyrosinase and mechanism of action.* J Biol Chem, 2002. **25**: p. 25.

136. Katsuki, O., *Skin Cosmetic.* Jpn Patent, 1994. **JP 06256150A**.

137. Shin, N.H., et al., *Oxyresveratrol as the potent inhibitor on dopa oxidase activity of mushroom tyrosinase.* Biochem Biophys Res Commun, 1998. **243**(3): p. 801-3.

138. Shin, N.H., et al., *Inhibitory effects of hydroxystilbenes on cyclooxygenase from sheep seminal vesicles.* Planta Med, 1998. **64**(3): p. 283-4.

139. Liu, B. and J.S. Hong, *Role of microglia in inflammation-mediated neurodegenerative diseases: mechanisms and strategies for therapeutic intervention.* J Pharmacol Exp Ther, 2003. **304**(1): p. 1-7.

140. Zamzami, N., et al., *Inhibitors of permeability transition interfere with the disruption of the mitochondrial transmembrane potential during apoptosis.* FEBS Lett, 1996. **384**(1): p. 53-7.

141. Zoratti, M. and I. Szabo, *Electrophysiology of the inner mitochondrial membrane.* J Bioenerg Biomembr, 1994. **26**(5): p. 543-53.

142. Longa, E.Z., et al., *Reversible middle cerebral artery occlusion without craniectomy in rats.* Stroke, 1989. **20**(1): p. 84-91.

143. Belayev, L., et al., *Middle cerebral artery occlusion in the rat by intraluminal suture. Neurological and pathological evaluation of an improved model.* Stroke, 1996. **27**(9): p. 1616-22; discussion 1623.

144. Bederson, J.B., et al., *Rat middle cerebral artery occlusion: evaluation of the model and development of a neurologic examination.* Stroke, 1986. **17**(3): p. 472-6.

145. Bederson, J.B., et al., *Evaluation of 2,3,5-triphenyltetrazolium chloride as a stain for detection and quantification of experimental cerebral infarction in rats.* Stroke, 1986. **17**(6): p. 1304-8.

146. Horn, T.F., et al., *Nitric oxide promotes intracellular calcium release from mitochondria in striatal neurons.* Faseb J, 2002. **16**(12): p. 1611-22.

147. Loupatatzis, C., et al., *Single-channel currents of the permeability transition pore from the inner mitochondrial membrane of rat liver and of a human hepatoma cell line.* Cell Physiol Biochem, 2002. **12**(5-6): p. 269-78.

148. Mongolsuk, S., A. Robertson, and R. Towers, *2:4:3':5'-Tetrahydroxystilbene from Artocarpus lakoocha.* J Org Chem, 1957: p. 2231-33.

149. Hirakura, K., et al., *Structures of Three New Natural Diels-Alder Type Adducts, Kuwanons P and X, and Mulberrofuran J, from the Cultivated Mulberry Tree (Morus Ihou KOIDZ.).* Chem Pharm Bull, 1985. **33**: p. 1088-96.

150. Qiu, F., et al., *A Novel Stilbene Glucoside, Oxyresveratrol 3'-O-β-Glucopyranoside, from the Root Bark of Morus alba.* Planta Med, 1996. **62**: p. 559-61.

151. Paxion, G. and C. Watson, *The Rat Brain in Stereotaxic Coordinates.* Academic Press, Sydney, 1986.

152. Ichas, F. and J.P. Mazat, *From calcium signaling to cell death: two conformations for the mitochondrial permeability transition pore. Switching from low- to high-conductance state.* Biochim Biophys Acta, 1998. **1366**(1-2): p. 33-50.

153. Fournier, N., G. Ducet, and A. Crevat, *Action of cyclosporine on mitochondrial calcium fluxes.* J Bioenerg Biomembr, 1987. **19**(3): p. 297-303.

154. Kowaltowski, A.J., R.F. Castilho, and A.E. Vercesi, *Mitochondrial permeability transition and oxidative stress.* FEBS Lett, 2001. **495**(1-2): p. 12-5.

155. Lorenz, P., et al., *Oxyresveratrol and resveratrol are potent antioxidants and free radical scavengers: effect on nitrosative and oxidative stress derived from microglial cells.* Nitric Oxide. **In Press, Corrected Proof**.

156. Reichert, S.A., J.S. Kim-Han, and L.L. Dugan, *The mitochondrial permeability transition pore and nitric oxide synthase mediate early mitochondrial depolarization in astrocytes during oxygen-glucose deprivation.* J Neurosci, 2001. **21**(17): p. 6608-16.

157. Smaili, S.S. and J.T. Russell, *Permeability transition pore regulates both mitochondrial membrane potential and agonist-evoked Ca2+signals in oligodendrocyte progenitors.* Cell Calcium, 1999. **26**(3-4): p. 121-130.

158. Fiskum, G., A.N. Murphy, and M.F. Beal, *Mitochondria in neurodegeneration: acute ischemia and chronic neurodegenerative diseases.* J Cereb Blood Flow Metab, 1999. **19**(4): p. 351-69.

159. Siesjo, B.K., *Pathophysiology and treatment of focal cerebral ischemia. Part I: Pathophysiology.* J Neurosurg, 1992. **77**(2): p. 169-84.

160. Siesjo, B.K., *Acid-base homeostasis in the brain: physiology, chemistry, and neurochemical pathology.* Prog Brain Res, 1985. **63**: p. 121-54.

161. Hansen, A.J. and T. Zeuthen, *Extracellular ion concentrations during spreading depression and ischemia in the rat brain cortex.* Acta Physiol Scand, 1981. **113**(4): p. 437-45.

162. Simon, R.P., et al., *Calcium overload in selectively vulnerable neurons of the hippocampus during and after ischemia: an electron microscopy study in the rat.* J Cereb Blood Flow Metab, 1984. **4**(3): p. 350-61.

163. Matsumoto, S., et al., *Restricted clinical efficacy of cyclosporin A on rat transient middle cerebral artery occlusion.* Life Sci, 2002. **72**(4-5): p. 591-600.

164. Matsumoto, S., et al., *Blockade of the mitochondrial permeability transition pore diminishes infarct size in the rat after transient middle cerebral artery occlusion.* J Cereb Blood Flow Metab, 1999. **19**(7): p. 736-41.

165. Nakatsuka, H., et al., *Release of cytochrome c from mitochondria to cytosol in gerbil hippocampal CA1 neurons after transient forebrain ischemia.* Brain Res, 1999. **849**(1-2): p. 216-9.

166. Liu, W., et al., *Kainate excitotoxicity in organotypic hippocampal slice cultures: evidence for multiple apoptotic pathways.* Brain Research, 2001. **916**(1-2): p. 239-248.

167. Ferrand-Drake, M., et al., *Cyclosporin A prevents calpain activation despite increased intracellular calcium concentrations, as well as translocation of apoptosis-inducing factor, cytochrome c and caspase-3 activation in neurons exposed to transient hypoglycemia.* J Neurochem, 2003. **85**(6): p. 1431-42.

168. Jiang, D., et al., *Zn(2+) induces permeability transition pore opening and release of pro-apoptotic peptides from neuronal mitochondria.* J Biol Chem, 2001. **276**(50): p. 47524-9.

169. Cassarino, D.S., et al., *The parkinsonian neurotoxin MPP+ opens the mitochondrial permeability transition pore and releases cytochrome c in isolated mitochondria via an oxidative mechanism.* Biochim Biophys Acta, 1999. **1453**(1): p. 49-62.

170. Li, P., et al., *Cytochrome c and dATP-dependent formation of Apaf-1/caspase-9 complex initiates an apoptotic protease cascade.* Cell, 1997. **91**(4): p. 479-489.

171. Kunduzova, O.R., et al., *Prevention of apoptotic and necrotic cell death, caspase-3 activation, and renal dysfunction by melatonin after ischemia/reperfusion.* Faseb J, 2003. **17**(8): p. 872-4.

172. Shen, Y.X., et al., *Melatonin blocks rat hippocampal neuronal apoptosis induced by amyloid beta-peptide 25-35.* J Pineal Res, 2002. **32**(3): p. 163-7.

173. Yoo, Y.M., et al., *Melatonin suppresses NO-induced apoptosis via induction of Bcl-2 expression in PGT-beta immortalized pineal cells.* J Pineal Res, 2002. **33**(3): p. 146-50.

174. Harms, C., et al., *Melatonin is protective in necrotic but not in caspase-dependent, free radical-independent apoptotic neuronal cell death in primary neuronal cultures.* Faseb J, 2000. **14**(12): p. 1814-24.

175. Krohn, A.J., T. Wahlbrink, and J.H. Prehn, *Mitochondrial depolarization is not required for neuronal apoptosis.* J Neurosci, 1999. **19**(17): p. 7394-404.

176. Hortnagl, H., et al., *Cholinergic deficit induced by ethylcholine aziridinium (AF64A) in rat hippocampus: effect on glutamatergic systems.* Naunyn Schmiedebergs Arch Pharmacol, 1991. **344**(2): p. 213-9.

177. Chung, S.-Y. and S.-H. Han, *Melatonin attenuates kainic acid-induced hippocampal neurodegeneration and oxidative stress through microglial inhibition.* J Pineal Res, 2003. **34**(2): p. 95-102.

178. Cuzzocrea, S., et al., *Protective effects of melatonin in ischemic brain injury.* J Pineal Res, 2000. **29**(4): p. 217-27.

179. Kilic, E., et al., *Pinealectomy aggravates and melatonin administration attenuates brain damage in focal ischemia.* J Cereb Blood Flow Metab, 1999. **19**(5): p. 511-6.

180. Reiter, R.J., *The ageing pineal gland and its physiological consequences.* Bioessays, 1992. **14**(3): p. 169-75.

181. Pennartz, C.M., et al., *Diurnal modulation of pacemaker potentials and calcium current in the mammalian circadian clock.* Nature, 2002. **416**(6878): p. 286-90.

182. Laing, R.J., J. Jakubowski, and R.W. Laing, *Middle cerebral artery occlusion without craniectomy in rats. Which method works best?* Stroke, 1993. **24**(2): p. 294-7; discussion 297-8.

183. Leker, R.R., et al., *Drug-induced hypothermia reduces ischemic damage: effects of the cannabinoid HU-210.* Stroke, 2003. **34**(8): p. 2000-6.

184. Bhalla, A., C.D. Wolfe, and A.G. Rudd, *Management of acute physiological parameters after stroke.* Qjm, 2001. **94**(3): p. 167-72.

185. Oh, H., et al., *Hepatoprotective and free radical scavenging activities of prenylflavonoids, coumarin, and stilbene from Morus alba.* Planta Med, 2002. **68**(10): p. 932-4.

186. Nakashima, M.N., et al., *Time course of nitric oxide synthase activity in neuronal, glial, and endothelial cells of rat striatum following focal cerebral ischemia.* Cell Mol Neurobiol, 1995. **15**(3): p. 341-9.

187. Ryu, J., et al., *Thrombin induces NO release from cultured rat microglia via protein kinase C, mitogen-activated protein kinase, and NF-kappa B.* J Biol Chem, 2000. **275**(39): p. 29955-9.

188. Faraci, F.M. and J.E. Brian, Jr., *Nitric oxide and the cerebral circulation.* Stroke, 1994. **25**(3): p. 692-703.

189. Chung, K.O., et al., *In-vitro and in-vivo anti-inflammatory effect of oxyresveratrol from Morus alba L.* J Pharm Pharmacol, 2003. **55**(12): p. 1695-700.

190. Chakraborti, T., et al., *Oxidant, mitochondria and calcium: an overview.* Cell Signal, 1999. **11**(2): p. 77-85.

191. Petrosillo, G., F.M. Ruggiero, and G. Paradies, *Role of reactive oxygen species and cardiolipin in the release of cytochrome c from mitochondria.* Faseb J, 2003. **17**(15): p. 2202-8.

192. Sugawara, T., et al., *Overexpression of copper/zinc superoxide dismutase in transgenic rats protects vulnerable neurons against ischemic damage by blocking the mitochondrial pathway of caspase activation.* J Neurosci, 2002. **22**(1): p. 209-17.

193. Jemmerson, R., et al., *A conformational change in cytochrome c of apoptotic and necrotic cells is detected by monoclonal antibody binding and mimicked by association of the native antigen with synthetic phospholipid vesicles.* Biochemistry, 1999. **38**(12): p. 3599-609.

194. Namura, S., et al., *Ebselen reduces cytochrome c release from mitochondria and subsequent DNA fragmentation after transient focal cerebral ischemia in mice.* Stroke, 2001. **32**(8): p. 1906-11.

8. LIST OF ABBREVIATIONS

ADP	Adenosine diphosphate
AIF	Apoptosis inducing factor
AMP	Adenosine monophosphate
AMPA	α-amino-3-hydroxy-5-methyl-4-isoxalone propionic acid
ANT	Adenine nucleotide translocase
Apaf-1	Apoptotic protease-activating factor-1
ATP	Adenosine triphosphate
BAX	Bcl_2 associated protein X
BGlu	Blood glucose
CAD	Caspase activated DNase
CBF	Cerebral blood flow
CsA	Cyclosporine A
Cu\Zn SOD	Copper \ zinc superoxide dismutase
DMEM	Dulbecco's modified Eagle's medium
ER	Endoplasmic reticulum
F0 F1-ATP	F0 F1-ATP synthase
FCS	Fetal calf serum
H_2O_2	Hydrogen peroxide
HBSS	Hepes buffered salt solution
Hct	Hematocrit
ICAD	Inhibitor of caspase activated DNase
MAP-2	Microtubule associated protein 2
MABP	Mean arterial blood pressure
MCA	Middle cerebral artery
MCAO	Middle cerebral artery occlusion
MDR	Multi drug resistance pump
Mel	Melatonin
MeValCsA	N-methyl-valine-4-cyclosporine A
Mn-SOD	Manganese superoxide dismutase
mtPTP	Mitochondrial permeability transition pore

NeuN	Neuronal nuclear protein
NFkB	Nuclear factor kappa B
NO	Nitric oxide
NOS	Nitric oxide synthase
NMDA	N-methyl-D-aspartate
NMR	Nuclear magnetic resonance
OGD	Oxygen-glucose deprivation
$^{\cdot}OH$	Hydroxyl radical
$O_2^{\cdot -}$	Superoxide anion
$ONOO^-$	Peroxynitrite
OMM	Outer mitochondrial membrane
OXY	Oxyresveratrol
PARP	Poly (ADP ribose) polymerase
PBS	Phosphate buffered saline
PFA	Para formaldehyde
ROS	Reactive oxygen species
RNS	Reactive nitrogen species
SOD	Superoxide dismutase
SPMA	Spontaneous motor activity
ssDNA	Single stranded DNA
VDAC	Voltage-dependent anionic channel